Discrete and Continuous Dynamical Systems - Series B

doi:10.3934/dcdsb.2023178

NON-CONFORMING MULTISCALE FINITE ELEMENT METHOD FOR STOKES FLOWS IN HETEROGENEOUS MEDIA. PART II: ERROR ESTIMATES FOR PERIODIC MICROSTRUCTURE

Gaspard Jankowiak[1] and Alexei Lozinski[*2]

[1]University of Konstanz, 78457 Konstanz, Germany

[2]Université de Franche-Comté, CNRS, LmB, F-25000 Besançon, France

(Communicated by Grégoire Allaire)

Abstract. This paper is dedicated to the rigorous numerical analysis of a Multiscale Finite Element Method (MsFEM) for the Stokes system, when dealing with highly heterogeneous media, as proposed in *B.P. Muljadi et al., Non-conforming multiscale finite Element method for Stokes flows in heterogeneous media. Part I: Methodologies and numerical experiments*, SIAM MMS (2015), **13**(4) 1146-–1172. The method is in the vein of the classical Crouzeix-Raviart approach. It is generalized here to arbitrary sets of weighting functions used to enforce continuity across the mesh edges. We provide error bounds for a particular set of weighting functions in a periodic setting, using an accurate estimate of the homogenization error. Numerical experiments demonstrate an improved accuracy of the present variant with respect to that of Part I, both in the periodic case and in a broader setting.

1. **Introduction.** We consider the Stokes problem in the perforated domain $\Omega^\varepsilon := \Omega \setminus B^\varepsilon$, $\Omega \subset \mathbb{R}^2$: find $u : \Omega^\varepsilon \to \mathbb{R}^2$ and $p : \Omega^\varepsilon \to \mathbb{R}$, solution of

$$-\Delta u + \nabla p = f \quad \text{on } \Omega^\varepsilon\,, \tag{1}$$

$$\operatorname{div} u = 0 \quad \text{on } \Omega^\varepsilon\,, \tag{2}$$

$$u = 0 \quad \text{on } \partial\Omega^\varepsilon\,, \tag{3}$$

where $f : \Omega \to \mathbb{R}^2$ is a given function, assumed sufficiently regular on Ω.

We are interested in the situations where the perforations B^ε have a complex structure, making a direct numerical solution of problem (1)–(3) very expensive. Typically, B^ε is assumed to be a set of obstacles of average size and average inter-obstacle distance $\varepsilon \ll diam(\Omega)$, so that the mesh resolving all the features of the perforated domain Ω^ε is too complex. Our goal is to devise an efficient numerical method that employs a relatively coarse mesh of size $H \geq \varepsilon$ (or even $H \gg \varepsilon$). We borrow the concept of Multiscale Finite Element Method (MsFEM) [25, 16], where the multiscale basis functions are pre-calculated on each cell of the coarse mesh, using a local sufficiently fine mesh, to represent a typical behavior of the

2020 *Mathematics Subject Classification.* Primary: 65N12; Secondary: 65N30, 35J15.

Key words and phrases. Crouzeix-Raviart Element, Multiscale Finite Element Method, Stokes Equations, Homogenization.

*Corresponding author: Alexei Lozinski.

microscopic structure of the flow. The global approximation to the solution of the problem in Ω^ε is then constructed as the Galerkin projection on the space spanned by these basis functions.

The particular variant of MsFEM pursued in this article is inspired by classical non-conforming Crouzeix-Raviart finite elements [11]. The idea of Crouzeix-Raviart MsFEM was first developed in [29, 30] for diffusion problems either with highly oscillating coefficients or posed on a perforated domain. It was also extended to advection-diffusion problems in [12] and to Stokes equation in the Part I of the present paper [32]. In the construction of Crouzeix-Raviart multiscale basis functions, the conformity between coarse elements is not enforced in a strong sense. The basis functions are required to be continuous only in a weak (finite element) sense, i.e. merely the averages of the jumps of these functions vanish at coarse element edges. The boundary conditions at the edges are then provided by a natural decomposition of the entire functional space into the sum of unresolved fine scales and the finite set of multiscale base functions. In the present article, we generalize this idea by introducing the weights into the averages over the edges in the definition of the functional spaces. This additional flexibility allows us to construct a more accurate variant of Crouzeix-Raviart MsFEM, as confirmed by the numerical experiments at the end of this article. Moreover, we are now able to provide a rigorous *a priori* error bounds in terms of H and ε in a periodic setting, i.e. when B^ε is populated by the same pattern repeated periodically on a grid of size ε. Note that a generalization to higher order weights (without a theoretical error analysis) as well as to the Oseen problem, and the corresponding implementation in *TrioCFD* (`http://triocfd.cea.fr/`) is presented in [18].

Let us mention briefly other approaches which can be applied to similar problems: wavelet-based homogenization method [13], variational multiscale method [33], equation-free computations [28], heterogeneous multiscale method [14] and many others. For viscous, incompressible flows, multiscale methods based on homogenization theory for solving slowly varying Stokes flow in porous media have been studied in [9, 8]. Returning to the MsFEM-type approaches, we should mention a big amount of work on the oversampling approach, first introduced in the original work [25] to provide a better approximation of the edge boundary condition of the multiscale basis functions. Oversampling here means that the local problem in the coarse element is extended to a domain larger than the element itself, but only the interior information would be communicated to the coarse scale equation. Various extensions of the sampled domain lead to various oversampling methods, cf. [16, 10, 23, 15]. Although an oversamping-based MsFEM for the Stokes equation is a possible direction of future research, we choose not to introduce the oversampling in this article. This is motivated by the numerical comparison between the Crouzeix-Raviart MsFEM and oversampling based approaches in [30] for *diffusion problems on perforated domains* demonstrating that the Crouzeix-Raviart MsFEM outperforms all the other variants.

This paper is organized as follows. The Crouzeix-Raviart MsFEM is presented in Section 2. We recall there namely the construction from Part I [32] and explain and motivate some modifications and generalization we make to this construction here. We also announce there the main theoretical result of the paper: an a priori error bound in the case of periodic perforations. The rest of the paper (with the exception of some numerical experiments) is constrained to this periodic setting.

Section 3 deals with the homogenization theory. We prove there an estimate of the error committed by the approximation of the Stokes equations with the Darcy ones. Section 4 deals with some technical lemmas. Section 5 presents the proof of the MsFEM error bound. Finally, the numerical tests are reported in Section 6.

2. MsFEM *à la* Crouzeix-Raviart.

We assume henceforth that Ω is a polygonal domain. We define a mesh $\mathcal{T}_H$ on Ω, i.e. a decomposition of Ω into polygons, each of diameter at most H, and denote $\mathcal{E}_H$ the set of all the edges of $\mathcal{T}_H$, $\mathcal{E}_H^{int} \subset \mathcal{E}_H$ the internal edges and $\mathcal{E}(T)$ the set of edges of $T \in \mathcal{T}_H$. Note that we mesh Ω and not the perforated domain Ω^ε. This allows us to use coarse elements (independently of the fine scales present in the geometry of Ω^ε) and leaves us with a lot of flexibility: some mesh nodes may be in B^ε, and likewise some edges may intersect B^ε.

We assume that the mesh does not have any hanging nodes, i.e. each internal edge is shared by exactly two mesh cells. In addition, $\mathcal{T}_H$ is assumed to be quasi-uniform in the following sense: fixing a polygon $\overline{T} \subset \mathbb{R}^2$ as reference element (one can also have a finite collection of reference elements), for any mesh element $T \in \mathcal{T}_H$, there exists a smooth invertible mapping $K : \overline{T} \to T$ such that $\|\nabla K\|_{L^\infty} \leq CH$, $\|\nabla K^{-1}\|_{L^\infty} \leq CH^{-1}$, C being some universal constant independent of T, which we will refer to as the regularity parameter of the mesh. To avoid some technical complications, we also assume that the mapping K is affine on every edge of $\partial\overline{T}$. These assumptions are obviously met by a triangular mesh satisfying the minimum angle condition (see e.g. [6, Section 4.4]), but our approach carries over to quadrangles, which are in fact used for our numerical computations, or to general polygonal meshes (in the flavor of Virtual Finite Elements [4]).

We shall use the usual notations $L^2(\omega)$, $H^k(\omega)$ for Sobolev spaces on a domain ω. We shall also denote $L^2_0(\omega) = \left\{p \in L^2(\omega) : \int_\omega p = 0\right\}$ and $H^1_0(\omega) = \{u \in H^1(\omega) : u|_{\partial\omega} = 0\}$. We shall implicitly identify the functions in $H^1_0(\Omega^\varepsilon)$ with those in $H^1(\Omega)$ vanishing on B^ε. The weak form of (1)–(3) can be written as follows: find $(u,p) \in H^1_0(\Omega^\varepsilon)^2 \times L^2_0(\Omega^\varepsilon)$ such that

$$c((u,p),(v,q)) = \int_\Omega f \cdot v, \quad \forall (v,q) \in H^1_0(\Omega^\varepsilon)^2 \times L^2_0(\Omega^\varepsilon)$$

with

$$c\left((u,p),(v,q)\right) := \int_{\Omega^\varepsilon} \nabla u : \nabla v - \int_{\Omega^\varepsilon} p \operatorname{div} v - \int_{\Omega^\varepsilon} q \operatorname{div} u\,. \tag{4}$$

We shall also need the broken Sobolev spaces of the type

$$H^1(\mathcal{T}_H) = \left\{u \in L^2(\Omega) : u|_T \in H^1(T) \text{ for any } T \in \mathcal{T}_H\right\}.$$

The partial derivatives $\partial_i u$ of a function u from $H^1(\mathcal{T}_H)$ will be understood in the piecewise sense, i.e. $\partial_i u$ will be assumed to coincide on any mesh cell $T \in \mathcal{T}_H$ with the distributional derivative of $u|_T$ in $\mathcal{D}(T)$. In particular, the H^1 semi-norm of a function $u \in H^1(\mathcal{T}_H)$ space will be understood as $|u|_{H^1(\Omega)} = \left(\sum_{T\in\mathcal{T}_H} |u|^2_{H^1(T)}\right)^{1/2}$. In the sequel, for the sake of simplicity, we will denote the norms on vector valued spaces in the same manner as for scalar values spaces.

The idea of the Multiscale Finite Element Method (MsFEM) *à la* Crouzeix-Raviart is to require the continuity of the finite element functions, which here are highly oscillatory, in the sense of some weighted averages on the edges. We have adapted this approach to the Stokes equation in [32] using the simplest possible

set of weights on the edges. We are now going to recall the main ideas of this construction and to generalize it to arbitrary weighting functions.

2.1. **Functional spaces.** Let us fix a positive integer s and associate some vector-valued functions $\omega_{E,1}, \dots, \omega_{E,s} : E \to \mathbb{R}^2$ to any edge $E \in \mathcal{E}_H$. As in [32], we first introduce the extended velocity space

$$V_H^{ext} := \left\{ \begin{array}{l} u \in L^2(\Omega)^2 \text{ such that } u|_T \in H^1(T)^2 \text{ for any } T \in \mathcal{T}_H, \\ u = 0 \text{ on } B^\varepsilon, \text{ and } \int_E [[u]] \cdot \omega_{E,j} = 0 \text{ for all } E \in \mathcal{E}_H, \ j = 1, \dots, s \end{array} \right\},$$

where $[[u]]$ denotes the jump of u across an internal edge and $[[u]] = u$ on the boundary $\partial\Omega$. The idea behind this space is to enhance the natural velocity space $H_0^1(\Omega^\varepsilon)^2$ so that we have at our disposal the vector fields discontinuous across the edges of the mesh. Indeed, our aim is to construct a nonconforming approximation method, where the continuity of the solution on the mesh edges will be preserved only for the weighted averages. We shall need some technical requirements on the weights:

Assumption 2.1. *For any $E \in \mathcal{E}_H$, $\mathrm{span}(\omega_{E,1} \dots, \omega_{E,s}) \ni n_E$, the unit normal to E.*

Note that the original construction from [32] is recovered by setting the weights as $s = 2$, $\omega_{E,1} = e_1 = \begin{pmatrix} 1 \\ 0 \end{pmatrix}$, $\omega_{E,2} = e_2 = \begin{pmatrix} 0 \\ 1 \end{pmatrix}$ on all the edges. Assumption 2.1 is then trivially verified. This will be also the case for another choice of the weights introduced later in this article.

The following assumptions deal not only with the weights but also with the manner in which the holes B_ε intersect the mesh cells.

Assumption 2.2. *Take any $T \in \mathcal{T}_H$ and any real numbers $c_1^E, \dots, c_s^E$ on all the edges E composing ∂T. There exists $v \in H^1(T)^2$ vanishing on $T \cap B^\varepsilon$ and such that $\int_E v \cdot \omega_{E,i} = c_i^E$, $i = 1, \dots, s$ for all the edges E.*

Assumption 2.3. *For any $T \in \mathcal{T}_H$, let $C_1, \dots, C_n$ be the connected components of $T \cap \Omega^\varepsilon$ and choose any real numbers $c_1, \dots, c_n$ with $\sum_{i=1}^n c_i = 0$. There exists $w \in H^1(T)^2$ vanishing on $T \cap B^\varepsilon$ and such that $\int_{\partial C_i} w \cdot n = c_i$, $i = 1, \dots, n$ and $\int_F w \cdot \omega_{F,j} = 0$ for all the edges F of T and $j = 1, \dots, s$.*

Remark 1.

1. Assumption 2.2 above will be valid provided the weights $\omega_{E,1}, \dots, \omega_{E,s}$ are linearly independent as functions on $E \setminus B^\varepsilon$. In particular, no edge E should be covered completely by B^ε. Note that the situations where some edges E are covered by B^ε can be easily handled by a slight modification of the forthcoming MsFEM method, cf. Lemma 2.4: one should simply ignore such edges when constructing the MsFEM basis functions.
2. Assumption 2.3 on the other hand may impose some restrictions on the choice of the mesh with respect to the perforations. However, it will be satisfied in most typical situations. First of all, we emphasize that this Assumption is void if $T \cap \Omega^\varepsilon$ is connected (one has then $n = 1$, $c_1 = 0$, and one puts $w = 0$). Moreover, the required function w can be easily constructed if, for example, a mesh element T is split by B^ε into two connected components C_1, C_2 and one of its edges, say E, is split into two non-empty connected components, say

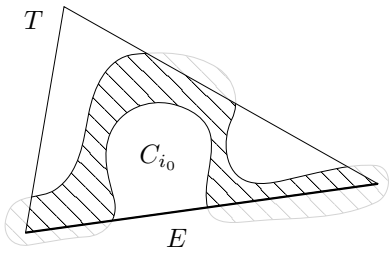

FIGURE 1. A typical situation where Assumption 2.3 does not hold. The fluid domain $T \cap \Omega^\varepsilon$ is in white and the edge E is in bold.

E_{C_1}, E_{C_2}: one can prescribe then the required non-zero averages of normal fluxes of w on E_{C_1} and E_{C_2} while letting $w \cdot n$ equal to 0 on the remaining parts of the boundary of C_1 and C_2. Similar constructions can be imagined in other more complicated situations.

3. A situation where Assumption 2.3 is not fulfilled is illustrated in Fig. 1. We have there $n = 3$ connected components (it can be generalized to any $n \geq 3$) and one of them, say the connected component C_{i_0}, intersects exactly one edge E, which itself does not intersect any other connected component: there is $1 \leq i_0 \leq n$ with $E \cap (\cup_i C_i) = C_{i_0}$ and $C_{i_0} \cap \partial T \subset E$. One can then choose $c_{i_0} > 0$. Any w fulfilling the requirements is such that $\int_{\partial C_{i_0}} w \cdot n = \int_{E \cap C_{i_0}} w \cdot n = \int_E w \cdot n = c_{i_0} > 0$. This is clearly incompatible with the condition $\int_E w \cdot \omega_{E,j} = 0$ for all j, in view of Assumption 2.1.

We introduce now the combined velocity-pressure space $X_H^{ext} = V_H^{ext} \times M$, with $M = L^2_0(\Omega^\varepsilon) := \left\{p \in L^2(\Omega^\varepsilon) \text{ s.t. } \int_{\Omega^\varepsilon} p = 0\right\}$. The space X_H^{ext} is then decomposed into coarse and fine components:

$$X_H^{ext} = X_H \oplus X_H^0 \,, \tag{5}$$

where $X_H^0 = V_H^0 \times M_H^0$ is the space of unresolved fine scales with

$$V_H^0 := \left\{ u \in V_H^{ext} : \int_E u \cdot \omega_{E,j} = 0 \quad \forall E \in \mathcal{E}_H,\ j = 1, \ldots, s \right\},$$
$$M_H^0 := \left\{ p \in M : \int_{T \cap \Omega^\varepsilon} p = 0 \quad \forall T \in \mathcal{T}_H \right\},$$

and X_H is chosen as the "orthogonal" complement of X_H^0 with respect to c, the natural bilinear form (4) associated to the Stokes problem:

$$(\vec{u}_H, p_H) \in X_H \iff c((\vec{u}_H, p_H), (\vec{v}, q)) = 0, \quad \forall (\vec{v}, q) \in X_H^0 \,. \tag{6}$$

We have put the word "orthogonal" in quotes since the bilinear form c is not a scalar product. We shall see however that the subspace $X_H \subset X_H^{ext}$ defined by (6) is finite-dimensional and forms indeed a direct sum with X_H^0, as announced in (5). This will be clear from the forthcoming Lemma 2.4. The space X_H in (6) will be referred to as the Crouzeix-Raviart MsFEM space and used to construct an approximation method.

An examination of the orthogonality relation (6) permits us to construct a basis of X_H in a localized manner, i.e. the support of every basis functions will cover a

small number of mesh cells, as in the standard finite element shape functions. To this end, we define the functional spaces $M_H \subset M$ and $V_H \subset V_H^{ext}$ as

$$M_H = \{q \in L_0^2(\Omega^\varepsilon) \text{ such that } q|_{T\cap\Omega^\varepsilon} = const,\ \forall T \in \mathcal{T}_H\}\,, \tag{7}$$

$$V_H = \text{span}\{\Phi_{E,i},\ E \in \mathcal{E}_H^{int},\ i = 1,\dots,s\}\,, \tag{8}$$

where $\Phi_{E,i}$ for any $E \in \mathcal{E}_H^{int}$, $i = 1,\dots,s$ is the vector-valued function on Ω, vanishing outside the two mesh cells T_1, T_2 adjacent to E, and defined on these two cells together with the accompanying pressure $\pi_{E,i}$ as the solution to the following problems: for $k = 1, 2$, find $\Phi_{E,i} \in H^1(T_k)^2$ s.t. $\Phi_{E,i} = 0$ on $T_k \cap B^\varepsilon$, $\pi_{E,i} \in L_0^2(T_k \cap \Omega^\varepsilon)$, and $\lambda_{F,j} \in \mathbb{R}$ for all $F \in \mathcal{E}(T_k)$, $j = 1,\dots,s$ such that

$$\int_{T_k\cap\Omega^\varepsilon} \nabla\Phi_{E,i} : \nabla v - \int_{T_k\cap\Omega^\varepsilon} \pi_{E,i}\,\text{div}\, v - \int_{T_k\cap\Omega^\varepsilon} q\,\text{div}\,\Phi_{E,i} + \sum_{j=1}^{s}\sum_{F\in\mathcal{E}(T_k)} \lambda_{F,j}\int_F v\cdot\omega_{F,j} = 0\,, \tag{9}$$

$$\int_F \Phi_{E,i}\cdot\omega_{F,j} = \delta_{ij}\delta_{EF} := \begin{cases} \delta_{ij},\ F = E \\ 0,\ F \neq E \end{cases}\,, \tag{10}$$

for all $v \in H^1(T_k \cap \Omega^\varepsilon)^2$ s.t. $v|_{T_k\cap B^\varepsilon} = 0$, $q \in L_0^2(T_k \cap \Omega^\varepsilon)$, and for all $F \in \mathcal{E}(T_k)$, $j = 1,\dots,s$. The unknowns $\lambda_{F,j}$ in (9) serve as the Lagrange multipliers for the constraints (10).

Remark 2. In the strong form, problem (9) can be rewritten as: find $\Phi_{E,i}$ and $\pi_{E,i}$ that solve on T_k, $k = 1, 2$

$$\begin{aligned}
-\Delta\Phi_{E,i} + \nabla\pi_{E,i} &= 0, && \text{on } \Omega^\varepsilon \cap T_k,\\
\text{div}\,\Phi_{E,i} &= const, && \text{on } \Omega^\varepsilon \cap T_k,\\
\Phi_{E,i} &= 0, && \text{on } B^\varepsilon \cap T_k,\\
\nabla\Phi_{E,i}n - \pi_{E,i}n &\in \text{span}\{\omega_{F,1},\dots,\omega_{F,s}\} && \text{on } F\cap\Omega^\varepsilon, \quad \text{for all } F \in \mathcal{E}(T_k),\\
\int_F \Phi_{E,i}\cdot\omega_{F,j} &= \delta_{ij}\delta_{EF} && \text{for all } F \in \mathcal{E}(T_k),\ j = 1,\dots,s\,,\\
\int_{\Omega^\varepsilon\cap T_k} \pi_{E,i} &= 0.
\end{aligned}$$

The functions $(\Phi_{E,i}, \pi_{E,i})$, together with the piecewise constants for the pressure, form indeed a basis of the Crouzeix-Raviart MsFEM space X_H. We make this precise in the following

Lemma 2.4. *Under Assumptions 2.1–2.3 the problems above are well posed and the MsFEM space X_H from (6) can be identified with*

$$X_H = \text{span}\{(u_H, \pi_H(u_H) + \bar{p}_H),\ u_H \in V_H,\ \bar{p}_H \in M_H\}\,, \tag{11}$$

where $\pi_H : V_H \to \text{span}\{\pi_{E,i},\ E \in \mathcal{E}_H^{int},\ i = 1, 2\} \subset M_H^0$ is the linear mapping such that $\pi_H(\Phi_{E,i}) = \pi_{E,i}$ for all $E \in \mathcal{E}_H^{int}$, $i = 1, 2$.

Proof. The well-posedness of problem (9) on any mesh element T_k (denoted simply by T in the sequel of this proof) follows from Assumption 2.2, which ensures that

one can prescribe the needed values to $\int_F \Phi_{E,i}\cdot\omega_{F,j}$ on all the edges F of element T_k, and from the following inf-sup condition

$$\inf_{q\in L^2_0(T\cap\Omega^\varepsilon)}\sup_{v\in V_{\int 0}(T)}\frac{\int_{T\cap\Omega^\varepsilon} q\,\mathrm{div}\, v}{\|q\|_{L^2(T\cap\Omega^\varepsilon)}|v|_{H^1(T)}}>0\,, \tag{12}$$

with

$$V_{\int 0}(T)=\{v: H^1(T)^2 : \int_E v=0,\ \forall E\in\mathcal{E}(T) \text{ and } v=0 \text{ on } B^\varepsilon\cap T\}.$$

In turn, property (12) can be established thanks to Assumption 2.3. Indeed, this property is evident if $T\cap\Omega^\varepsilon$ is connected: given $q\in L^2_0(T\cap\Omega^\varepsilon)$ one takes then $v\in H^1_0(T\cap\Omega^\varepsilon)^2\subset V_{\int 0}(T)$ (assuming that v is extended by zero on B^ε) such that $\mathrm{div}\, v=q$ and the H^1 norm of v is bounded by the L^2 norm of q (the existence of such a function is assured by [20, Corollary 2.4, p.24]). If not, recall the connected components $C_1,\dots,C_n$ of $T\cap\Omega^\varepsilon$, denote $c_i=\int_{C_i} q$ for a given $q\in L^2_0(T\cap\Omega^\varepsilon)$, observe $\sum_{i=1}^n c_i=0$ and consider the function w from Assumption 2.3. We have $w\in V_{\int 0}(T)$ and

$$\int_{C_i}\mathrm{div}\, w=\int_{\partial C_i} w\cdot n=c_i=\int_{C_i} q\,.$$

One can now choose $w^{(i)}\in H^1_0(C_i)^2$ on each component C_i such that $\mathrm{div}\, w^{(i)}=q-\mathrm{div}\, w$ on C_i. Such functions exist thanks to the above mentioned result from [20] since $\int_{C_i}(q-\mathrm{div}\, w)=0$. Setting $v=w+w^{(i)}$ on C_i and $v=0$ on B^ε gives $v\in V_{\int 0}(T)$ such that $\mathrm{div}\, v=q$. By construction, the H^1 norm of v is bounded by the L^2 norm of q.

To prove the other statements of the proposition one can easily adapt the proofs of Lemmas 3.1, 3.2 and Remark 3.3 in [32] with obvious modifications induced by the more general constraints $\int_E[[u]]\cdot\omega_{E,j}=0$, replacing $\int_E[[u]]=0$ in the definition of V_H^{ext}. We shall not go into the details of these modifications for the sake of brevity. We emphasize only that Assumption 2.1 is indeed necessary to conclude. For example, the proof that $\int_{\Omega^\varepsilon}\bar p_H\,\mathrm{div}\, v=0$ for any $\bar p_H\in M_H$ and $v\in V_H^0$, cf. Lemma 3.1 in [32], goes like this

$$\int_{\Omega^\varepsilon}\bar p_H\,\mathrm{div}\, v=\sum_{T\in\mathcal{T}_H}\bar p_H|_T\int_T\mathrm{div}\, v=\sum_{T\in\mathcal{T}_H}\bar p_H|_T\int_{\partial T} v\cdot n=0\,.$$

The last equality above is justified by $\mathrm{span}(\omega_{E,1}\dots,\omega_{E,s})\supset n_E$ on any edge E of T. □

From now on, we can think of V_H as the finite dimensional space defined by (8). From this construction, we see easily that $\mathrm{div}(V_H)\subset M_H$. Indeed, $\mathrm{div}(v_H)$ is piecewise constant on $\mathcal{T}_H$ for any $v_H\in V_H$ and

$$\int_{\Omega^\varepsilon}\mathrm{div}\, v_H=\sum_{T\in\mathcal{T}_H}\int_T\mathrm{div}\, v_H=\sum_{E\in\mathcal{E}_H}\int_E[[v_H\cdot n_E]]=0\,.$$

In fact, $\mathrm{div}(V_H)=M_H$ as will be shown in Lemma 2.5.

2.2. **The MsFEM approximation.** The approximation of the solution to the Stokes problem (1)–(3) now reads: find $u_H \in V_H$ and $p_H \in M_H$ such that

$$\int_{\Omega^\varepsilon} \nabla u_H : \nabla v_H - \int_{\Omega^\varepsilon} p_H \operatorname{div} v_H = \int_{\Omega^\varepsilon} f \cdot v_H \quad \forall v_H \in V_H \,, \tag{13}$$

$$\int_{\Omega^\varepsilon} q_H \operatorname{div} u_H = 0 \qquad \forall q_H \in M_H \,, \tag{14}$$

Existence and uniqueness of the solution to (13)–(14) follows from the standard theory of saddle-point problems provided the pair of spaces $V_H \times M_H$ satisfies the inf-sup property. This is indeed the case, as shown in the next lemma.

Lemma 2.5. *Assume that the continuous velocity-pressure inf-sup property holds on Ω^ε with a constant $\beta > 0$, i.e.*

$$\inf_{p \in L^2_0(\Omega^\varepsilon)} \sup_{v \in H^1_0(\Omega^\varepsilon)^2} \frac{\int_{\Omega^\varepsilon} p \operatorname{div} v}{\|p\|_{L^2(\Omega^\varepsilon)} |v|_{H^1(\Omega^\varepsilon)}} \geq \beta \,.$$

Then, the discrete inf-sup property holds on $V_H \times M_H$ with the same constant $\beta > 0$:

$$\inf_{p_H \in M_H} \sup_{v_H \in V_H} \frac{\int_{\Omega^\varepsilon} p_H \operatorname{div} v_H}{\|p_H\|_{L^2(\Omega^\varepsilon)} |v_H|_{H^1(\Omega^\varepsilon)}} \geq \beta \,.$$

More precisely, for any $p_H \in M_H$ there exists $v_H \in V_H$ such that

$$\operatorname{div} v_H = p_H \ \text{ on } T \cap \Omega^\varepsilon, \ \forall T \in \mathcal{T}_H \quad \text{and} \quad |v_H|_{H^1(\Omega^\varepsilon)} \leq \frac{1}{\beta} \|p_H\|_{L^2(\Omega^\varepsilon)} \,.$$

Proof. Take arbitrary $p_H \in M_H$ and $v \in H^1_0(\Omega^\varepsilon)^2$ such that

$$\operatorname{div} v = p_H \text{ on } \Omega^\varepsilon \quad \text{and} \quad |v|_{H^1(\Omega^\varepsilon)} \leq \frac{1}{\beta} \|p_H\|_{L^2(\Omega^\varepsilon)} \,.$$

Decompose $v = v_H + v_H^0$ with $v_H \in V_H$ and $v_H^0 \in V_H^0$. Assuming that v is extended by 0 inside B^ε, this implies $\int_E v \cdot n_E = \int_E v_H \cdot n_E$ on any $E \in \mathcal{E}_H$ so that for any $T \in \mathcal{T}_H$

$$\int_{T \cap \Omega^\varepsilon} \operatorname{div} v_H = \int_{\partial T} v_H \cdot n = \int_{\partial T} v \cdot n = \int_{T \cap \Omega^\varepsilon} \operatorname{div} v = \int_{T \cap \Omega^\varepsilon} p_H \,.$$

Since both $\operatorname{div} v_H$ and p_H are piecewise constant on $\mathcal{T}_H$, we conclude $\operatorname{div} v_H = p_H$.

Moreover, $\int_{\Omega^\varepsilon} \nabla(v - v_H) : w_H = 0$ for any $w_H \in V_H$ by the construction of V_H, cf. the orthogonality between X_H and X_H^0. Hence $|v_H|_{H^1} \leq |v|_{H^1}$ which proves the Lemma. □

In fact, the velocity u_H given by (13)–(14) can be characterized in a simpler manner: find $u_H \in Z_H$ such that

$$\int_{\Omega^\varepsilon} \nabla u_H : \nabla v_H = \int_{\Omega^\varepsilon} f \cdot v_H, \quad \forall v_H \in Z_H \,, \tag{15}$$

where Z_H is the divergence free subspace of V_H:

$$Z_H = \{ u_H \in V_H \text{ such that } \operatorname{div} u_H = 0 \text{ on any } T \in \mathcal{T}_H \} \,. \tag{16}$$

This fact will be useful in the proof of the error estimate.

Remark 3. Our method can be easily adapted to non-homogeneous boundary conditions on the outer boundary $\partial\Omega$, i.e. when (3) is replaced with

$$u = g \text{ on } \partial\Omega \quad \text{and} \quad u = 0 \text{ on } \partial B^\varepsilon\,. \tag{17}$$

One should then add the following equations on all the mesh edges E lying on $\partial\Omega$:

$$\int_E u_H \cdot \omega_{E,j} = \int_E g \cdot \omega_{E,j}, \quad j = 1, \dots, s.$$

2.3. **Possible choices of weighting functions.** We now consider two choices of weighting functions, leading to 2 variants of multiscale spaces:

$$\mathrm{CR}_2 : s = 2,\ \omega_{E,1} = e_1,\ \omega_{E,2} = e_2, \tag{18}$$

$$\mathrm{CR}_3 : s = 3,\ \omega_{E,1} = e_1,\ \omega_{E,2} = e_2,\ \omega_{E,3} = n_E\psi_E, \tag{19}$$

for any $E \in \mathcal{E}_H$. Here n_E denote again a unit vector normal to E and ψ_E a linear polynomial on E such that $\int_E \psi_E = 0$. The actual choice of n_E and ψ_E should be made once for all, but is arbitrary otherwise.

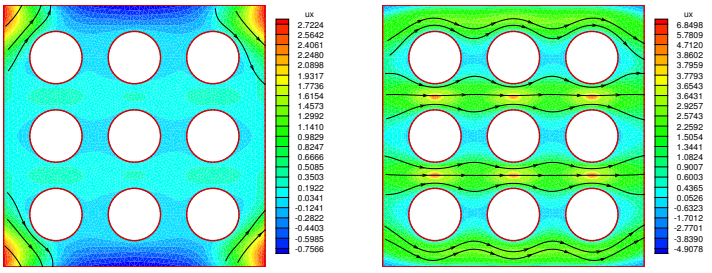

FIGURE 2. Basis function combination $\Phi_{LR} = \Phi_{L,1} + \Phi_{R,1}$. Left: Φ_{LR} computed with CR_2 basis functions (18); Right: Φ_{LR} computed with CR_3 basis functions (19). We show the stream-lines associated to these vector-valued functions. The colors represent their x-components.

We recognize the space CR_2 as being the MsFEM space from the Part I of the present series [32] where it was successfully tested numerically. It can however be quite inefficient in certain situations, especially when some of the mesh cells contain a lot of densely packed holes. Consider, for example, a geometrical configuration as in Fig. 2. We represent there a mesh cell (a square), say $T \in \mathcal{T}_H$, which happens to contain 9 round holes. We plot on the left the sum of basis functions $\Phi_{LR} := \Phi_{L,1} + \Phi_{R,1}$ from the CR_2 basis associated to the two vertical sides of T, L being the left side and R the right side of T and assuming that the unit normal is chosen in the direction e_1 on both edges L and R. We thus impose the flow to be (in average) in e_1 direction on both vertical sides of T and to vanish (in average again) on both horizontal sides. We consider a sum of basis functions, rather than a basis function alone, since $\mathrm{div}(\Phi_{LR}) = 0$ on T as $\int_T \mathrm{div}\,\Phi_{LR} = \int_R \Phi_{R,1} \cdot e_1 - \int_{L,1} \Phi_L \cdot e_1 = 0$, while $\int_T \mathrm{div}\,\Phi_{L,1} = const \neq 0$ there. The vector field Φ_{LR} should model, roughly speaking, the flow from left to right inside T. However, the actual behavior of Φ_{LR} is quite different and counter-intuitive: the fluid seems to turn around the corners

of the cell T, which have of course no physical meaning, and barely penetrates inside T between the obstacles. One concludes thus that the CR_2 space V_H cannot be used in general to construct a reasonable approximation of the solution to the Stokes problem. Turning to the alternative CR_3 space, we plot at Fig. 2 on the right the same linear combination $\Phi_{L,1} + \Phi_{R,1}$ of basis functions. We see now that their behavior is at least visually correct. The superiority of CR_3 over CR_2 will be further confirmed by other numerical experiments in Section 6. Moreover, we shall be able to prove an error estimate for the MsFEM approximation using the CR_3 basis functions, cf. Theorem 2.7 below and its proof in Section 5.

Remark 4. Following [30], one could think that the drawbacks of CR_2 basis functions could be fixed if one added appropriate multi-scale bubble functions to the CR_2 MsFEM space. One could thus introduce for any $T \in \mathcal{T}_H$ the vector-valued velocity bubble $\Psi_{T,i}$ with associated pressure $\theta_{T,i}$, $i = 1, 2$ with $\Psi_{T,i}$, $\theta_{T,i}$ supported in T and solution to

$$\begin{aligned}
-\Delta \Psi_{T,i} + \nabla \theta_{T,i} &= e_i && \text{on } \Omega^\varepsilon \cap T, \\
\operatorname{div} \Psi_{T,i} &= 0 && \text{on } \Omega^\varepsilon \cap T, \\
\Psi_{T,i} &= 0 && \text{on } B^\varepsilon \cap T, \\
\nabla \Psi_{T,i} n - \theta_{T,i} n &= const && \text{on } F \cap \Omega^\varepsilon \quad \text{for all } F \in \mathcal{E}(T), \\
\int_F \Psi_{T,i} &= 0 && \text{for all } F \in \mathcal{E}(T), \\
\int_{\Omega^\varepsilon \cap T} \theta_{T,i} &= 0\,.
\end{aligned}$$

We plot such a function at Fig. 3 in a setting similar to that of Fig. 2 and observe that it could indeed restore the typical flow features lacking in the CR_2 basis functions. However, CR_2 MsFEM space, even enhanced with such bubble functions, would perform poorly with respect to the non-conformity error inherent to our method, cf. Remark 6. This is why we have chosen not to consider the bubble functions in the present article, contrary to [30].

More general choices for the weighting functions, using higher order polynomials and eventually introducing some appropriate bubble functions, are proposed and tested numerically in [18, 19].

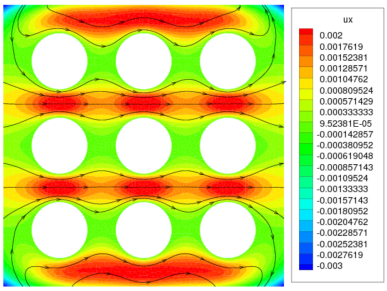

FIGURE 3. Bubble function $\Psi_{T,1}$ on the same mesh cell T as at Fig. 2.

2.4. **Periodic case.** The theoretical study of the MsFEM method introduced above will be performed only in the case of periodic perforations. Moreover, we need to be careful about the introduction of perforations near the boundary $\partial\Omega$. We adopt thus the following set of hypotheses.

Assumption 2.6. *$\Omega \in \mathbb{R}^2$ is a bounded simply connected polygonal domain, B^ε is a periodic set of holes inside Ω, described below, and $\Omega^\varepsilon = \Omega \setminus \bar{B}^\varepsilon$. Consider first the reference cell, the unit square $Y = (0,1)^2$, a domain $B \subset Y$ with sufficiently smooth boundary (the obstacle domain), and $\mathcal{F} = Y \setminus B$ (the fluid domain). Assume $dist(\partial B, \partial Y) > 0$ and $\mathcal{F}$ connected. Take $\varepsilon > 0$ and define for any $i \in \mathbb{Z}^2$: $Y_i = \varepsilon(Y + i)$, $B_i = \varepsilon(B + i)$, $\mathcal{F}_i = \varepsilon(\mathcal{F} + i)$. Finally, set*

$$\mathcal{I} = \{i \in \mathbb{Z}^2 : Y_i \subset \Omega\}, \quad B^\varepsilon = \cup_{i\in\mathcal{I}} B_i \text{ and } \Omega^\varepsilon = \Omega \setminus \bar{B}^\varepsilon.$$

These definitions are illustrated in Fig. 4. Note that our definition of the perforated domain is slightly different from that of [31], where Ω^ε is perforated by all B_i that are enclosed in Ω. Here, we only leave the holes B_i contained in a cell Y_i which is itself inside Ω.

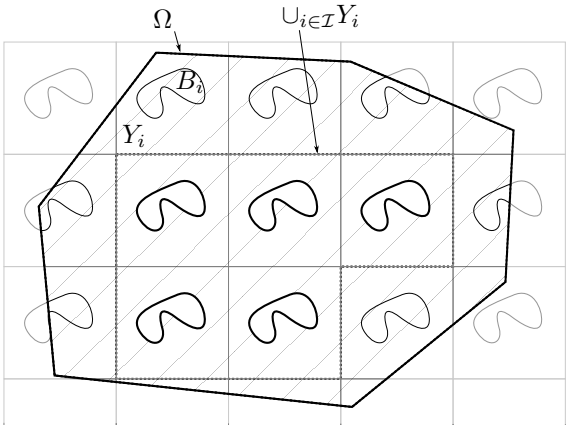

FIGURE 4. Domain setup, Ω^ε is crosshatched and its boundary is in bold lines

We can now announce our main result, i.e. the error estimate for the CR_3 MsFEM method.

Theorem 2.7. *Adopt Assumption 2.6 on the perforated domain Ω^ε and 2.2–2.3 about the mesh and the weighting functions used to set up the MsFEM method. Assume moreover that the weighting functions are chosen as in (19). Suppose also that f and the homogenized pressure p^*, cf. Section 3, are sufficiently smooth. The following error bound holds between the solution to the Stokes equations (1–3) and its MsFEM approximation (13)–(14)*

$$|u - u_H|_{H^1(\Omega)} + \varepsilon\|p - p_H\|_{L^2(\Omega)} \leq C\varepsilon\left(H + \sqrt{\varepsilon} + \sqrt{\frac{\varepsilon}{H}}\right)\left(\|f - \nabla p^*\|_{H^2(\Omega)\cap C^1(\bar{\Omega})} + |p^*|_{H^2(\Omega)}\right), \quad (20)$$

where the constant C depends only on the mesh regularity and the perforation pattern B.

The proof is postponed until Section 5 and will use the results on homogenization from the next section and some technical lemmas from Section 4. Note that the norms of both f and p^* are present in the right-hand side of (20). This is due to the low regularity assumption on $\partial\Omega$ (we only suppose that Ω is polygonal). If the boundary of Ω were sufficiently smooth, the norms of p^* could be bounded by the norm of f by the elliptic regularity estimates for problem (27)–(28).

3. Homogenization for Stokes in two dimensions.

3.1. The formal two-scale asymptotic expansion.

We want to derive the asymptotic equation corresponding to (1), in the limit $\varepsilon \to 0$ under Assumption 2.6 of periodic obstacles. Let us do it first formally by introducing the two-scale asymptotic expansions in terms of slow variable x and the fast variable $y = x/\varepsilon$. This procedure is quite well known, see for example [24, 35]. We describe it here for completeness and to set our notations. Let us expand u and p as

$$u(x) = \sum_{k\geq 2} \varepsilon^k u_k(x,y)\,, \qquad p(x) = \sum_{k\geq 0} \varepsilon^k p_k(x,y)\,, \qquad y = \frac{x}{\varepsilon}\,,$$

where all the functions u_k, p_k are assumed $\mathbb{Z}^2$-periodic in y, i.e. 1-periodic with respect to both y_1 and y_2. The fact that the expansion for u can be started at the order ε^2 and that of p at the order ε^0 can be justified by energy estimates. Without going into these details, we just observe that this choice allows us to obtain a closed system of equations for consecutive terms, as shown below.

We substitute these series into the Stokes equations, use the chain rule, and get in the leading order $\frac{1}{\varepsilon}$,

$$\nabla_y p_0 = 0 \quad \text{ on } \mathcal{F}\,.$$

This gives $p_0(x,y) = p^*(x)$.

At order ε^0 we get

$$\begin{aligned} -\Delta_y u_2 + \nabla_y p_1 &= f - \nabla_x p^* && \text{on } \mathcal{F}\,,\\ \operatorname{div}_y u_2 &= 0 && \text{on } \mathcal{F}\,,\\ u_2 &= 0 && \text{on } \partial B\,. \end{aligned}$$

Recalling that u_2 and p_1 are $\mathbb{Z}^2$-periodic in y, this gives that u_2 and p_1 are the linear combinations of the solutions to the following cell Stokes problems: for $i = 1, 2$ find $w_i : \mathcal{F} \to \mathbb{R}^2$ and $\pi_i : \mathcal{F} \to \mathbb{R}$, $\mathbb{Z}^2$-periodic and solution of

$$\begin{aligned} -\Delta w_i + \nabla \pi_i &= e_i && \text{on } \mathcal{F}\,,\\ \operatorname{div} w_i &= 0 && \text{on } \mathcal{F}\,,\\ w_i &= 0 && \text{on } \partial B\,,\\ \int_{\mathcal{F}} \pi_i &= 0\,. \end{aligned} \tag{21}$$

We have thus, employing from now on the Einstein convention of summation on repeating indices,

$$\begin{aligned} u_2(x,y) &= w_i(y)(f_i(x) - \partial_i p^*(x))\,,\\ p_1(x,y) &= \pi_i(y)(f_i(x) - \partial_i p^*(x))\,. \end{aligned} \tag{22}$$

The equation for $p^*(x)$ results from the next term in the asymptotic expansion, at order ε:

$$\begin{aligned} -\Delta_y u_3 + \nabla_y p_2 &= 2(\nabla_y \cdot \nabla_x) u_2 - \nabla_x p_1 && \text{on } \mathcal{F}\,, \\ \operatorname{div}_y u_3 &= -\operatorname{div}_x u_2 && \text{on } \mathcal{F}\,, \\ u_3 &= 0 && \text{on } \partial B\,, \end{aligned}$$

plus periodicity conditions. The total outward flux of u_3 on $\partial\mathcal{F}$ is zero in view of the boundary conditions, so that the system of equations above has a solution if and only if $\langle \operatorname{div}_x u_2 \rangle = 0$ where $\langle\cdot\rangle$ stands for the average over $\mathcal{F}$:

$$\langle v \rangle = \frac{1}{|\mathcal{F}|} \int_{\mathcal{F}} v(y)\, dy. \tag{23}$$

This gives Darcy's equation for p^*:

$$\operatorname{div}(\langle w_i \rangle (f_i - \partial_i p^*)) = 0 \quad \text{on } \Omega\,.$$

We see that u_3 and p_2 are the linear combinations of the solutions to yet another cell Stokes problem: for $i,j = 1,2$ find $\gamma_{ij} : \mathcal{F} \to \mathbb{R}^2$ and $\vartheta_{ij} : \mathcal{F} \to \mathbb{R}$, $\mathbb{Z}^2$-periodic and solution of

$$\begin{aligned} -\Delta \gamma_{ij} + \nabla \vartheta_{ij} &= 2\partial_j w_i - \pi_i e_j && \text{on } \mathcal{F}\,, \\ \operatorname{div} \gamma_{ij} &= -w_i \cdot e_j + \langle w_i \cdot e_j \rangle && \text{on } \mathcal{F}\,, \\ \gamma_{ij} &= 0 && \text{on } \partial B\,, \\ \int_{\mathcal{F}} \vartheta_{ij} &= 0\,. \end{aligned} \tag{24}$$

We have thus

$$\begin{aligned} u_3(x,y) &= \gamma_{ij}(y) \partial_j (f_i(x) - \partial_i p^*(x))\,, \\ p_2(x,y) &= \vartheta_{ij}(y) \partial_j (f_i(x) - \partial_i p^*(x))\,. \end{aligned} \tag{25}$$

From now on, we will denote by u^* the homogenized velocity, i.e. the first non-zero terms in the expansion of u:

$$u^* = \varepsilon^2 u_2(x,y) = \varepsilon^2 (w_i)_\varepsilon \left(f_i - \partial_i p^*\right)\,. \tag{26}$$

Notation. We use a shorthand $(\cdot)_\varepsilon$ to indicate the rescaling by ε. Thus, $(\phi)_\varepsilon(x) = \phi\left(\frac{x}{\varepsilon}\right)$ for any $\mathbb{Z}^2$ periodic function ϕ.

The procedure above does not provide boundary conditions for p^*. The good choice for these is to ensure that the normal component of the averaged homogenized velocity vanishes on the boundary, i.e. $n \cdot \langle u^* \rangle = 0$ on $\partial\Omega$.

3.2. **A rigorous homogenization estimate.** The homogenization of the Stokes equations was first rigorously studied in [37], where the weak L^2 convergence for the velocity and the strong L^2 convergence for the pressure were established. The strong L^2 convergence for the velocity was later proven in [1]. However, for our purposes, it is desirable to have a convergence result in H^1 and, moreover, an estimate of the homogenization error in this norm. Such an estimate is available in [31] with a relative error of order $\sqrt[6]{\varepsilon}$. We shall improve it here to $\sqrt{\varepsilon}$ and provide another approach to the proof (as already noted, our definition of the perforated domain is slightly different from that in [31]). Our homogenization result follows. Very recently, similar estimates have been also proven in [36] by a different approach: the proof of [36] goes by constructing the boundary layer correctors, whereas our

proof relies on a simpler cut-off argument. We also note that, unlike [36] and much of the preceding literature, we do not introduce a pressure reconstruction inside the holes B^ε; our estimate for the error in pressure is established in the fluid domain only. There is also some discrepancy in the settings between our results and those of [36]: the regularity assumption on the data f and on the smoothness of the boundary $\partial\Omega$ are not the same. In particular, we choose not to rely on an elliptic regularity argument to deduce the reularity of p^* from that of f since our theorem should be valid in polygonal domains. That is why p^* is kept in the right-hand side of our error estimates.

Theorem 3.1. *Recall Assumption 2.6 and let u, p be the solution to the Stokes equations (1)–(3), p^* be the solution to the Darcy equation*

$$\operatorname{div}(\langle w_i\rangle(f_i - \partial_i p^*)) = 0 \quad \text{on } \Omega\,, \tag{27}$$

$$n \cdot \langle w_i\rangle(f_i - \partial_i p^*) = 0 \quad \text{on } \partial\Omega\,, \tag{28}$$

and u^* be defined by (26) with w_i extended by 0 inside B. Assuming that f and p^* are sufficiently smooth and $\int_{\Omega^\varepsilon} p^* = 0$ there holds

$$\|p - p^*\|_{L^2(\Omega^\varepsilon)} \le C\varepsilon^{\frac{1}{2}} \|f - \nabla p^*\|_{H^2(\Omega)\cap C^1(\bar\Omega)}\,, \tag{29}$$

$$|u - u^*|_{H^1(\Omega^\varepsilon)} \le C\varepsilon^{\frac{3}{2}} \|f - \nabla p^*\|_{H^2(\Omega)\cap C^1(\bar\Omega)}\,, \tag{30}$$

$$\|u - u^*\|_{L^2(\Omega^\varepsilon)} \le C\varepsilon^{\frac{5}{2}} \|f - \nabla p^*\|_{H^2(\Omega)\cap C^1(\bar\Omega)}\,, \tag{31}$$

where C is independent of ε.

Remark 5. The estimate for the velocity in the H^1 norm essentially says that the relative error is of order $\sqrt{\varepsilon}$. Indeed, the velocity itself is of order ε^2, but its derivatives are of order ε since both the exact solution and its homogenized approximation oscillate on the length scale ε. Also note that the deterioration of order $\sqrt{\varepsilon}$ is due to the boundary layers near $\partial\Omega$. Indeed, u^* does not satisfy the boundary condition $u = 0$ on $\partial\Omega$, which worsens the approximation near the boundary. Technically, this is taken into account by the introduction of the cut-off function η^ε in the forthcoming proof. If the boundary layers were absent, which would be the case, for example, under the periodic boundary conditions over a rectangular box $\Omega = (0, \varepsilon n) \times (0, \varepsilon m)$ with $n, m \in \mathbb{N}$, the a priori error estimate would give the relative error of order ε. Indeed, inspecting the forthcoming proof, one can see that neither Lemma 3.3 nor the cut-off functions η^ε are no longer needed in this case and the final result becomes

$$\frac{1}{\varepsilon^2}\|u - u^*\|_{L^2(\Omega^\varepsilon)} + \frac{1}{\varepsilon}|u - u^*|_{H^1(\Omega)} + \|p - p^*\|_{L^2(\Omega^\varepsilon)} \le C\varepsilon \|f - \nabla p^*\|_{H^2(\Omega^\varepsilon)}\,.$$

First, let us establish two technical lemmas of the inf-sup type related to the divergence free constraint (Lemma 3.2) and to the boundary conditions for the velocity (Lemma 3.3). All these results are proved under Assumption 2.6.

Lemma 3.2. *For any $q \in L^2_0(\Omega^\varepsilon)$ there exists $v \in H^1_0(\Omega^\varepsilon)^2$ such that*

$$\operatorname{div} v = q \text{ on } \Omega^\varepsilon \text{ and } |v|_{H^1(\Omega^\varepsilon)} \le \frac{C}{\varepsilon}\|q\|_{L^2(\Omega^\varepsilon)}\,, \tag{32}$$

where $C > 0$ is a constant independent of ε.

Proof. Let us take any $q \in L^2_0(\Omega)$ such that $q = 0$ on B^ε. Using [20, Corollary 2.4, p.24], we can pick some $w \in H^1_0(\Omega)^2$ such that

$$\operatorname{div} w = q \text{ on } \Omega \text{ and } |w|_{H^1(\Omega)} \le C\|q\|_{L^2(\Omega)}. \tag{33}$$

This gives us a velocity field w on Ω that does not satisfy the boundary conditions on Ω^ε, i.e. $w \neq 0$ on ∂B^ε. Using it as a starting point, we can construct an admissible velocity field on each cell $\mathcal{F}_i$, proceeding cell by cell, as follows.

Let us pick any $i \in \mathcal{I}$, denote by w_{Y_i}, q_{Y_i} the restrictions of w, q to the cell Y_i and map them to the reference cell Y:

$$\hat{w}_Y(x) = w_{Y_i}(\varepsilon(x+i)), \quad \hat{q}_Y(x) = \varepsilon q_{Y_i}(\varepsilon(x+i)).$$

The scalings are chosen so that

$$\operatorname{div} \hat{w}_Y = \hat{q}_Y \text{ on } Y.$$

A standard trace theorem assures that there exists $r \in H^1(\mathcal{F})^2$ such that

$$r = \hat{w}_Y \text{ on } \partial Y, \quad r = 0 \text{ on } \partial B \quad \text{and} \quad \|r\|_{H^1(\mathcal{F})} \leq C\|\hat{w}_Y\|_{H^{\frac{1}{2}}(\partial Y)} \leq C\|\hat{w}_Y\|_{H^1(Y)}.$$

Using again the corollary from [20] mentioned above and noting that

$$\int_{\mathcal{F}} (\hat{q}_Y - \operatorname{div} r) = \int_{\mathcal{F}} \hat{q}_Y - \int_{\partial\mathcal{F}} r \cdot n = \int_Y \hat{q}_Y - \int_{\partial Y} \hat{w}_Y \cdot n = \int_Y (\hat{q}_Y - \operatorname{div} \hat{w}_Y) = 0\,,$$

we can construct $z \in H^1_0(\mathcal{F})^2$ with

$$\operatorname{div} z = \hat{q}_Y - \operatorname{div} r \text{ and } \|z\|_{H^1(\mathcal{F})} \leq C\|\hat{q}_Y - \operatorname{div} r\|_{L^2(\mathcal{F})} \leq C\|\hat{w}_Y\|_{H^1(Y)}.$$

Setting now $\hat{v}_Y \in H^1(\mathcal{F})^2$ as $\hat{v}_Y = r + z$ we observe

$$\hat{v}_Y = \hat{w}_Y \text{ on } \partial Y, \quad \hat{v}_Y = 0 \text{ on } \partial B, \quad \operatorname{div} \hat{v}_Y = \hat{q}_Y \text{ and } \|\hat{v}_Y\|_{H^1(\mathcal{F})} \leq C\|\hat{w}_Y\|_{H^1(Y)}.$$

Note that the constants C in the above bounds depend only on the geometry of $\mathcal{F}$. In particular, they are obviously ε-independent. We now rescale the cell Y back to the cell Y_i of size ε and define $v_{Y_i} \in H^1(F_i)^2$ by $\hat{v}_Y(x) = v_{Y_i}(\varepsilon(x+i))$. Recalling the scalings of the functions and of their norms

$$\begin{cases} \hat{v}_Y(x) = v_{Y_i}(\varepsilon(x+i)) \\ \hat{w}_Y(x) = w_{Y_i}(\varepsilon(x+i)) \\ \hat{q}_Y(x) = \varepsilon q_{Y_i}(\varepsilon(x+i)) \end{cases} \Rightarrow \begin{cases} |\hat{v}_Y|_{H^1} = |v_{Y_i}|_{H^1} \\ \|\hat{w}_Y\|_{H^1} = \left(|w_{Y_i}|^2_{H^1} + \dfrac{1}{\varepsilon^2}\|w_{Y_i}\|_{L^2}\right)^{\frac{1}{2}} \leq \dfrac{1}{\varepsilon}\|w_{Y_i}\|_{H^1}\,, \\ \|\hat{q}_Y\|_{L^2} = \|q_{Y_i}\|_{L^2} \end{cases}$$

we conclude

$$\operatorname{div} v_{Y_i} = q_{Y_i} \text{ on } \mathcal{F}_i,\ v_{Y_i} = w_{Y_i} \text{ on } \partial Y_i,\ v_{Y_i} = 0 \text{ on } \partial B_i\,, \tag{34}$$

and

$$|v_{Y_i}|_{H^1(\mathcal{F}_i)} \leq \frac{C}{\varepsilon}\|w_{Y_i}\|_{H^1(Y_i)}\,.$$

We now collect all the pieces v_{Y_i} into $v \in H^1_0(\Omega^\varepsilon)^2$ such that $v|_{Y_i} = v_{Y_i}$ for any cell Y_i, $i \in \mathcal{I}$ and let $v = w$ on $\Omega_b := \Omega \setminus \cup_{i\in\mathcal{I}} Y_i$. Such a function v meets all the requirements of the lemma. Indeed, $\operatorname{div} v = q$ on Ω^ε and

$$\begin{aligned} |v|^2_{H^1(\Omega^\varepsilon)^2} &= |w|^2_{H^1(\Omega_b)} + \sum_{i\in\mathcal{I}} |v_{Y_i}|^2_{H^1(\mathcal{F}_i)} \\ &\leq |w|^2_{H^1(\Omega_b)} + \sum_{i\in\mathcal{I}} \frac{C}{\varepsilon^2}\|w\|^2_{H^1(Y_i)} \leq \frac{C}{\varepsilon^2}\|w\|^2_{H^1(\Omega)} \leq \frac{C}{\varepsilon^2}\|q\|^2_{L^2(\Omega^\varepsilon)}\,. \end{aligned}$$

□

Lemma 3.2 is very close to the results on the restriction operator in [37, 26]. Our next result is essentially taken from [31] but we provide here a slightly simpler construction that suits well to polygonal domains.

Lemma 3.3. *For any $g \in C^1(\bar\Omega)^2$ with $\operatorname{div} g = 0$ on Ω, $g\cdot n = 0$ on $\partial\Omega$, $\delta > 0$ small enough, there exists $v \in H^1(\Omega)^2$ such that $\operatorname{supp} v \subset O^\delta := \{x \in \Omega : dist(x, \partial\Omega) < \delta\}$ and*

$$v = g \text{ on } \partial\Omega, \quad \operatorname{div} v = 0 \text{ on } \Omega, \text{ and } |v|_{H^1(\Omega)} \le \frac{C}{\sqrt{\delta}} \|g\|_{C^1(\bar\Omega)},$$

where $C > 0$ is a constant independent of δ.

Proof. According to [20, Theorem 3.1], we can write $g = \nabla^\perp \Psi$ for some $\Psi \in H^1(\Omega)$, with $\nabla^\perp = (-\partial_2, \partial_1)^T$. In fact, $\Psi \in C^2(\bar\Omega)$ as seen from the explicit construction

$$\Psi(x) = -\int_a^x g^\perp \cdot d\vec{R},$$

where x is any point in Ω, a is a fixed point in Ω, $g^\perp = (-g_2, g_1)^T$ and the integral is taken over any curve connecting a and x (parameterized by a vector function $\vec{R}$). Note that $g \cdot n = \nabla\Psi \cdot \tau = 0$ on $\partial\Omega$, where n (resp. τ) is the unit vector normal (resp. tangent) to $\partial\Omega$, so we can choose Ψ such that $\Psi(x) = 0$ on $\partial\Omega$. We can now pick a cut-off function $\eta \in C^\infty(\Omega)$ such that $\eta(x) = 1$ on $O^{\delta/2}$, $\eta(x) = 0$ on $\Omega \setminus O^\delta$, and $\|\nabla\eta\|_{L^\infty} \le \frac{C}{\delta}$, $\|\nabla^2\eta\|_{L^\infty} \le \frac{C}{\delta^2}$. Here and below, C stands for positive constants independent of δ. Now, setting $v = \nabla^\perp(\eta\Psi)$, we have $\operatorname{div} v = 0$, $\operatorname{supp} v \subset O^\delta$, $v = g$ on $\partial\Omega$, and

$$\begin{aligned}
|v|_{H^1(\Omega)} &= \|\nabla\nabla^\perp(\eta\Psi)\|_{L^2(O^\delta)} \\
&\le \|\eta\nabla\nabla^\perp\Psi\|_{L^2(O^\delta)} + 2\|(\nabla\eta)(\nabla^\perp\Psi)\|_{L^2(O^\delta)} + \|\Psi\nabla\nabla^\perp\eta\|_{L^2(O^\delta)} \\
&\le C\|\nabla g\|_{L^2(O^\delta)} + \frac{C}{\delta}\|g\|_{L^2(O^\delta)} + \frac{C}{\delta^2}\|\Psi\|_{L^2(O^\delta)} \\
&\le C\sqrt{\delta}\|\nabla g\|_{L^\infty(\Omega)} + \frac{C}{\sqrt{\delta}}\|g\|_{L^\infty(\Omega)} + \frac{C}{\delta^{3/2}}\|\Psi\|_{L^\infty(O^\delta)}
\end{aligned}$$

since $\operatorname{meas}(O^\delta) \le C\delta$. We observe now that any point $x \in O^\delta$ can be connected to a point $y \in \partial\Omega$ by a segment of length no greater than δ lying in O^δ. Recalling that $\Psi(y) = 0$ and using the Taylor expansion of order 0 gives $|\Psi(x)| \le \delta|\nabla\Psi(z)|$ for some point z lying on this segment. Thus,

$$\|\Psi\|_{L^\infty(O^\delta)} \le \delta\|\nabla\Psi\|_{L^\infty(O^\delta)} = \delta\|g\|_{L^\infty(\Omega)},$$

which yields the result. □

We remind also a Poincaré inequality on the perforated domain.

Lemma 3.4. *Under Assumption 2.6, for any $\phi \in H^1_0(\Omega^\varepsilon)$*

$$\|\phi\|_{L^2(\Omega^\varepsilon)} \le C\varepsilon|\phi|_{H^1(\Omega^\varepsilon)}, \tag{35}$$

with a constant $C > 0$ independent of ε.

Proof. This is a corollary of Lemma 4.6 proven below. The present lemma can be also proven directly, cf. for example [24] or [30, Appendix A.1]. The definition of the perforated domain in these references is slightly different from the present article (the perforations are maintained near the boundary) but this does not change essentially the proof, since the band where the perforations are eliminated is of width $\sim \varepsilon$. □

Proof of Theorem 3.1. Consider

$$w_i' = w_i - |\mathcal{F}|\,\langle w_i\rangle = w_i - \int_Y w_i,$$

with w_i extended by 0 inside B and observe that $\operatorname{div} w_i' = 0$ on Y (in the sense of distributions), w_i' is $\mathbb{Z}^2$-periodic and of zero mean over Y. Thus (cf. [27, p. 6]) there exists a $\mathbb{Z}^2$-periodic function ψ_i such that

$$w_i - |\mathcal{F}|\langle w_i\rangle = \nabla^\perp \psi_i \text{ on } Y\,.$$

In fact, ψ_i can be assumed as smooth on $\mathcal{F}$ as we want, as seen from its explicit construction

$$\psi_i(x) = \int_0^1 (x_2[w_i']_1(tx) - x_1[w_i']_2(tx))\; dt\,,$$

and the fact that w_i is smooth thanks to our assumptions on perforation B.

Assumptions 2.6 also implies that there exists a constant $c > 0$ such that O^δ with $\delta = c\varepsilon$ does not intersect the holes $\cup_{i\in\mathcal{I}} B_i$ (here, O^δ stands for the band of width δ near $\partial\Omega$ as in Lemma 3.3). Let us choose a cut-off function $\eta^\varepsilon \in C^\infty(\bar\Omega)$ with $\eta^\varepsilon = \frac{\partial \eta^\varepsilon}{\partial n} = 0$ on $\partial\Omega$, $\eta^\varepsilon(x) = 1$ on $\Omega \setminus O^\delta$ and

$$\|\eta^\varepsilon\|_{L^\infty(\Omega)} = 1,\ \|1-\eta^\varepsilon\|_{L^2(\Omega)} \le C\sqrt{\varepsilon},\ |\eta^\varepsilon|_{H^1(\Omega)} \le \frac{C}{\sqrt{\varepsilon}},\ |\eta^\varepsilon|_{H^2(\Omega)} \le \frac{C}{\varepsilon^{3/2}}\,. \quad (36)$$

We now consider the expansion of the velocity of order 3 in ε and correct it using the cut-off η^ε to take into account the boundary layer:

$$\begin{aligned} u^{\varepsilon,3} = {}& \varepsilon^2|\mathcal{F}|\langle w_i\rangle(f_i - \partial_i p^*) + \varepsilon^3\nabla^\perp((\psi_i)_\varepsilon\eta^\varepsilon)(f_i - \partial_i p^*) \\ & + \varepsilon^3(\gamma_{ij})_\varepsilon\eta^\varepsilon\partial_j(f_i - \partial_i p^*)\,. \end{aligned} \quad (37)$$

The lower index $(\cdot)_\varepsilon$ is used here and below according to Notation on page 13. We also assume that γ_{ij} are extended by 0 inside B so that $u^{\varepsilon,3}$ is well defined on the whole of Ω. Remind that $\eta^\varepsilon = 1$ on $\Omega\setminus O^\delta$ so that the expression for $u^{\varepsilon,3}$ simplifies on this portion of Ω to

$$u^{\varepsilon,3} = u^* + \varepsilon^3 u_3 = \varepsilon^2(w_i)_\varepsilon(f_i - \partial_i p^*) + \varepsilon^3(\gamma_{ij})_\varepsilon\partial_j(f_i - \partial_i p^*)\,. \quad (38)$$

It means in particular that $u^{\varepsilon,3}$ vanishes on the holes B_i, $i\in\mathcal{I}$ which are all inside $\Omega\setminus O^\delta$. Let us compute $\operatorname{div} u^{\varepsilon,3}$ knowing that the divergence of the first term in (37) vanishes by (27):

$$\begin{aligned} \operatorname{div} u^{\varepsilon,3} = {}& \varepsilon^2(\nabla^\perp\psi_i)_\varepsilon\eta^\varepsilon\cdot\nabla(f_i - \partial_i p^*) + \varepsilon^3(\psi_i)_\varepsilon\nabla^\perp\eta^\varepsilon\cdot\nabla(f_i - \partial_i p^*) \\ & + \varepsilon^2(\operatorname{div}\gamma_{ij})_\varepsilon\eta^\varepsilon\partial_j(f_i - \partial_i p^*) \\ & + \varepsilon^3(\gamma_{ij})_\varepsilon\cdot(\nabla\eta^\varepsilon)\partial_j(f_i - \partial_i p^*) + \varepsilon^3(\gamma_{ij})_\varepsilon\eta^\varepsilon\cdot\nabla\partial_j(f_i - \partial_i p^*)\,. \end{aligned}$$

Grouping together the terms of order ε^2, using equation (24) for $\operatorname{div}\gamma_{ij}$, and denoting by G_ε all the terms of order ε^3, namely

$$\begin{aligned} G_\varepsilon := {}& \varepsilon^3(\psi_i)_\varepsilon\nabla^\perp\eta^\varepsilon\cdot\nabla(f_i - \partial_i p^*) \\ & + \varepsilon^3(\gamma_{ij})_\varepsilon\cdot(\nabla\eta^\varepsilon)\partial_j(f_i - \partial_i p^*) + \varepsilon^3(\gamma_{ij})_\varepsilon\eta^\varepsilon\cdot\nabla\partial_j(f_i - \partial_i p^*)\,, \end{aligned}$$

we proceed with the calculation as

$$\begin{aligned} \operatorname{div} u^{\varepsilon,3} &= \varepsilon^2\eta^\varepsilon(w_i - |\mathcal{F}|\langle w_i\rangle - (w_i - \langle w_i\rangle))_\varepsilon\cdot\nabla(f_i - \partial_i p^*) + G_\varepsilon \\ &= \varepsilon^2\eta^\varepsilon|B|\operatorname{div}(\langle w_i\rangle(f_i - \partial_i p^*)) + G_\varepsilon = G_\varepsilon\,. \end{aligned}$$

Note that this equality also holds trivially inside any hole B_k, $k\in\mathbb{Z}^2$ since both sides vanish there. Thanks to the bounds (36), we conclude

$$\|G_\varepsilon\|_{L^2(\Omega^\varepsilon)} \le C\varepsilon^{\frac{5}{2}}\|f - \nabla p^*\|_{H^2(\Omega)\cap C^1(\bar\Omega)}\,,$$

with $C > 0$ independent of ε. We also note for future use

$$u - u^{\varepsilon,3} = g := -\varepsilon^2 |\mathcal{F}| \langle w_i \rangle (f_i - \partial_i p^*) \text{ on } \partial\Omega\,. \tag{39}$$

We now turn to estimates for the residual in (1) caused by the homogenization. One of the technical difficulties consists in the presence of "virtual" holes B_i near $\partial\Omega$ that are in fact in the fluid domain Ω^ε according to our conventions, cf. Assumption 2.6 and Fig. 4 (the gray hole contours in the periodic cells cut by the boundary $\partial\Omega$). One should thus define properly the cell velocities w_i inside B_k. The usual extension by 0, which worked fine in all the previous calculations, does not suffice here because it does not give a twice differentiable function. We thus introduce an extension $\tilde{w}_i$ of w_i from $\mathcal{F}$ to Y such that $\tilde{w}_i = w_i$ on $\mathcal{F}$ and $\tilde{w}_i$ is of class C^2 on Y. Now, consider

$$\tilde{u}^* = \varepsilon^2 (\tilde{w}_i)_\varepsilon \, (f_i - \partial_i p^*)\ .$$

Similarly, let $\tilde{\pi}_i$ be an extension of π_i from $\mathcal{F}$ to Y such that $\tilde{\pi}_i = \pi_i$ on $\mathcal{F}$ and $\tilde{\pi}_i$ is of class C^1 on Y. Introduce the expansion of first order in ε for the pressure

$$\tilde{p}^{\varepsilon,1} = p^* + \varepsilon (\tilde{\pi}_i)_\varepsilon (f_i - \partial_i p^*)\,. \tag{40}$$

Thus, the residual due to the homogenization in eq. (1) is given everywhere on Ω^ε by

$$\begin{aligned} F_\varepsilon &:= -\Delta(u - \tilde{u}^*) + \nabla(p - \tilde{p}^{\varepsilon,1}) \\ &= f + (\Delta \tilde{w}_i - \nabla \tilde{\pi}_i)_\varepsilon (f_i - \partial_i p^*) \\ &\quad + 2\varepsilon (\nabla \tilde{w}_i)_\varepsilon \nabla (f_i - \partial_i p^*) + \varepsilon^2 (\tilde{w}_i)_\varepsilon \Delta (f_i - \partial_i p^*) \\ &\quad - \nabla p^* - \varepsilon (\tilde{\pi}_i)_\varepsilon \nabla (f_i - \partial_i p^*)\,. \end{aligned} \tag{41}$$

Rearranging the terms yields

$$\begin{aligned} F_\varepsilon = {} & 2\varepsilon (\nabla \tilde{w}_i)_\varepsilon \nabla (f_i - \partial_i p^*) + \varepsilon^2 (\tilde{w}_i)_\varepsilon \Delta (f_i - \partial_i p^*) - \varepsilon (\tilde{\pi}_i)_\varepsilon \nabla (f_i - \partial_i p^*) \\ & + (\Delta \tilde{w}_i - \nabla \tilde{\pi}_i + e_i)_\varepsilon (f_i - \partial_i p^*)\,. \end{aligned}$$

The terms in the first line above are of order ε or higher. The terms in the second line are of order 1, but they vanish in fact at all the fluid cells $\mathcal{F}_i$, $i \in \mathcal{I}$. Since the measure of the remaining part $\Omega^\varepsilon \setminus \cup_{i\in\mathcal{I}} \mathcal{F}_i$ is of order ε, we get

$$\|F_\varepsilon\|_{L^2(\Omega^\varepsilon)} \le C\sqrt{\varepsilon} \|f - \nabla p^*\|_{H^2(\Omega)\cap C^1(\bar{\Omega})}\,. \tag{42}$$

We summarize all the derived bounds as follows: the functions $u - \tilde{u}^*, u - u^{\varepsilon,3} \in H^1(\Omega^\varepsilon)^2$ and $p - \tilde{p}^{\varepsilon,1} \in L^2(\Omega^\varepsilon)$ satisfy

$$\begin{aligned} -\Delta(u - \tilde{u}^*) + \nabla(p - \tilde{p}^{\varepsilon,1}) &= F_\varepsilon \quad && \text{on } \Omega^\varepsilon\,, \\ \operatorname{div}(u - u^{\varepsilon,3}) &= G_\varepsilon \quad && \text{on } \Omega_\varepsilon\,, \\ u - u^{\varepsilon,3} &= 0 \quad && \text{on } \partial B^\varepsilon\,, \\ u - u^{\varepsilon,3} &= g \quad && \text{on } \partial\Omega\,. \end{aligned} \tag{43}$$

Apart from the difference between $\tilde{u}^*$ and $u^{\varepsilon,3}$, this is a Stokes system and we proceed with bounding the norms of its solution in the standard manner, cf. [20], using the inf-sup Lemmas 3.2 and 3.3. Indeed, Lemma 3.2 assures that there exists $v_p \in H^1_0(\Omega^\varepsilon)^2$ such that

$$\operatorname{div} v_p = G_\varepsilon \text{ and } |v_p|_{H^1(\Omega^\varepsilon)} \le \frac{C}{\varepsilon} \|G_\varepsilon\|_{L^2(\Omega^\varepsilon)} \le C\varepsilon^{\frac{3}{2}} \|f - \nabla p^*\|_{H^2(\Omega)\cap C^1(\bar{\Omega})}\,.$$

Recall that O^δ with $\delta = c\varepsilon$ as introduced above, does not intersect B^ε. Then, in view of the definition of g (39) and equations (27)–(28), Lemma 3.3 assures that there exists $v_b \in H^1(\Omega^\varepsilon)^2$ supported in O^δ and thus vanishing on B^ε such that $\operatorname{div} v_b = 0$ on Ω^ε,

$$v_b = g \text{ on } \partial\Omega \text{ and } |v_b|_{H^1(\Omega_\varepsilon)} \leq \frac{C}{\sqrt{\varepsilon}}\|g\|_{C^1(\bar\Omega)} \leq C\varepsilon^{\frac{3}{2}}\|f - \nabla p^*\|_{C^1(\bar\Omega)}\,.$$

Set $v = u - u^{\varepsilon,3} - v_p - v_b$ and observe that $v \in H^1_0(\Omega_\varepsilon)^2$ and $\operatorname{div} v = 0$ on Ω^ε. Multiplying (43) by v and integrating over Ω^ε by parts yields

$$\int_{\Omega^\varepsilon} \nabla(u - \tilde u^*) : \nabla v = \int_{\Omega^\varepsilon} F_\varepsilon \cdot v \leq \|F_\varepsilon\|_{L^2(\Omega^\varepsilon)}\|v\|_{L^2(\Omega^\varepsilon)} \leq C\varepsilon\|F_\varepsilon\|_{L^2(\Omega^\varepsilon)}|v|_{H^1(\Omega^\varepsilon)}\,.$$

We have used here Poincaré inequality (35) with $\phi = v$. Thus,

$$\begin{aligned}|v|^2_{H^1(\Omega^\varepsilon)} &\leq C\varepsilon\|F_\varepsilon\|_{L^2(\Omega^\varepsilon)}|v|_{H^1(\Omega^\varepsilon)} - \int_{\Omega_\varepsilon} \nabla(u^{\varepsilon,3} + v_p + v_b - \tilde u^*) : \nabla v \\ &\leq \left(C\varepsilon\|F_\varepsilon\|_{L^2(\Omega^\varepsilon)} + |\tilde u^* - u^{\varepsilon,3}|_{H^1(\Omega^\varepsilon)} + |v_p|_{H^1(\Omega^\varepsilon)} + |v_b|_{H^1(\Omega^\varepsilon)}\right)|v|_{H^1(\Omega^\varepsilon)}\,.\end{aligned}$$

We observe

$$\tilde u^* - u^* = \varepsilon^2(\tilde w_i - w_i)_\varepsilon\,(f_i - \partial_i p^*)$$

and

$$u^* - u^{\varepsilon,3} = -\varepsilon^3(\psi_i)_\varepsilon(\nabla^\perp\eta^\varepsilon)(f_i - \partial_i p^*) - \varepsilon^3(\gamma_{ij})_\varepsilon\eta^\varepsilon\partial_j(f_i - \partial_i p^*)\,,$$

which entails $|\tilde u^* - u^*|_{H^1(\Omega^\varepsilon)} \leq C\varepsilon^{\frac{3}{2}}\|f - \nabla p^*\|_{C^1(\bar\Omega)}$ since $\tilde w_i - w_i$ vanishes in Ω^ε outside of a band near $\partial\Omega$ of width of order ε, and finally $|\tilde u^* - u^{\varepsilon,3}|_{H^1(\Omega^\varepsilon)} \leq C\varepsilon^{\frac{3}{2}}\|f - \nabla p^*\|_{H^2(\Omega)\cap C^1(\bar\Omega)}$ thanks to the bounds (36). Combining this with (42) and the above estimates on v_p and v_b proves

$$|v|_{H^1(\Omega^\varepsilon)} \leq C\varepsilon^{\frac{3}{2}}\|f - \nabla p^*\|_{H^2(\Omega)\cap C^1(\bar\Omega)}\,,$$

and consequently (30) by the triangle inequality. The L^2 estimate (31) follows thanks to (35).

To prove the remaining estimate for pressure (29), we take $v \in H^1_0(\Omega^\varepsilon)$ such that $\operatorname{div} v = p - \tilde p^{\varepsilon,1}$ as constructed in Lemma 3.2, multiply (43) by v and integrate by parts

$$\begin{aligned}&\int_{\Omega^\varepsilon}(p - \tilde p^{\varepsilon,1})^2 = \int_{\Omega^\varepsilon}(p - \tilde p^{\varepsilon,1})\operatorname{div} v = \int_{\Omega^\varepsilon} F_\varepsilon \cdot v - \int_{\Omega^\varepsilon}\nabla(u - \tilde u^*) : \nabla v \\ &\leq C\varepsilon^{\frac{3}{2}}\|f - \nabla p^*\|_{H^2(\Omega)\cap C^1(\bar\Omega)}|v|_{H^1(\Omega^\varepsilon)} \leq C\varepsilon^{\frac{1}{2}}\|f - \nabla p^*\|_{H^2(\Omega)\cap C^1(\bar\Omega)}\|p - \tilde p^{\varepsilon,1}\|_{L^2(\Omega^\varepsilon)}\,.\end{aligned}$$

using the estimate in Lemma 3.2. Thus, by the triangle inequality,

$$\|p - p^*\|_{L^2(\Omega^\varepsilon)} \leq \|p - \tilde p^{\varepsilon,1}\|_{L^2(\Omega^\varepsilon)} + \|\tilde p^{\varepsilon,1} - p^*\|_{L^2(\Omega^\varepsilon)} \leq C\varepsilon^{\frac{1}{2}}\|f - \nabla p^*\|_{H^2(\Omega)\cap C^1(\bar\Omega)}\,,$$

since $(\tilde p^{\varepsilon,1} - p^*)$ term is of order ε as seen from (40).

4. **Technical lemmas.**

We assume implicitly in this section that mesh $\mathcal{T}_H$ is quasi-uniform, as described in the beginning of Section 2 and that Assumptions 2.2-2.3 and 2.6 are valid. The weights w_i are assumed to be chosen as in (19), i.e. we only study the CR_3 variant of the method.

4.1. **Some lemmas borrowed from the usual finite element theory.** The results collected in this section are well known. We emphasize however that they are valid on general polygonal meshes, which is a setting different form that of the standard textbooks, like [6, 17].

Lemma 4.1. *For all $T \in \mathcal{T}_H$, all the edges $E \subset \partial T$ and all $v \in H^1(T)$*

$$\|v\|^2_{L^2(E)} \leq C\left(H^{-1}\|v\|^2_{L^2(T)} + H\|\nabla v\|^2_{L^2(T)}\right). \tag{44}$$

Proof. This is the standard trace inequality properly scaled to a domain of diameter $\sim H$.The exact value of the constant C is given in Theorem 1.5.1.10 of [21]. □

Lemma 4.2. *Let Π_H be the $L^2(\Omega)$-orthogonal projection on the space of piecewise constant functions on $\mathcal{T}_H$. For any $f \in H^1(\Omega)$,*

$$\|f - \Pi_H f\|_{L^2(\Omega)} \leq CH|f|_{H^1(\Omega)} \tag{45}$$

holds with a constant $C > 0$ depending only on the regularity of $\mathcal{T}_H$.

Proof. This is a standard finite element interpolation result. It is proven by a Poincaré inequality on the reference element and scaling. If all the mesh cells are convex, one can take $C = 1/\pi$, cf. [3]. □

Lemma 4.3. *There exists a bounded linear operator $I_H : H^1(\Omega) \to H^1(\Omega)$ such that $I_H v$ is a polynomial of degree ≤ 1 on any edge $E \in \mathcal{E}_H$ for any $v \in H^1(\Omega)$ and it holds*

$$\|I_H v - v\|_{L^2(\Omega)} \leq CH|v|_{H^1(\Omega)}.$$

Moreover, if $v \in H^2(\Omega)$,

$$|I_H v - v|_{H^1(\Omega)} \leq CH|v|_{H^2(\Omega)}$$

holds with a constant $C > 0$ depending only on the regularity of $\mathcal{T}_H$.

Proof. One can simply take I_H as the usual Clément interpolation operator on P_1 finite elements if $\mathcal{T}_H$ is a triangular mesh. Otherwise, we consider $\widehat{\mathcal{T}}_H$ a submesh of $\mathcal{T}_H$ which consists of triangles only. To construct $\widehat{\mathcal{T}}_H$, one only needs to remesh the reference element $\overline{T}$ in triangles, without adding nodes on $\partial\overline{T}$. Applying the mapping K on each element of $\mathcal{T}_H$ one obtains then $\widehat{\mathcal{T}}_H$. We can now define I_H as the Clément interpolation operator on P_1 finite elements on $\widehat{\mathcal{T}}_H$. □

4.2. **Lemmas related to perforated domains and oscillating functions.**

Lemma 4.4. *Suppose $H \geq \gamma\varepsilon$ with some big enough γ. Let $T \subset \mathcal{T}_H$ and take any $v \in H^1(T)^2$ vanishing on $B^\varepsilon \cap T$. Then,*

$$\|v\|_{L^2(\partial T)} \leq C\sqrt{\varepsilon}|v|_{H^1(T)}. \tag{46}$$

holds. The constants $\gamma > 0$ and $C > 0$ here depend only on the regularity of mesh $\mathcal{T}_H$ and on the perforation pattern B.

Proof. We can safely suppose that the perforation pattern B contains a disc of radius $c_1 > 0$. It means that each perforation εB_k, $k \in \mathbb{Z}^2$ contains a disc of radius $r_0 = c_1\varepsilon$. As shown in Fig. 5, the boundary ∂T can be decomposed into non overlapping segments $S^0, S^1, S^2 \ldots$ such that each segment S lies at a distance no greater than $c_2\varepsilon$ from the center of a disc of radius r_0 which lies completely inside $B^\varepsilon \cap T$. In order to do this, we should suppose that the mesh cell is big enough, hence the restriction $H \geq \gamma\varepsilon$. Thus, to each segment S we associate a disc of radius

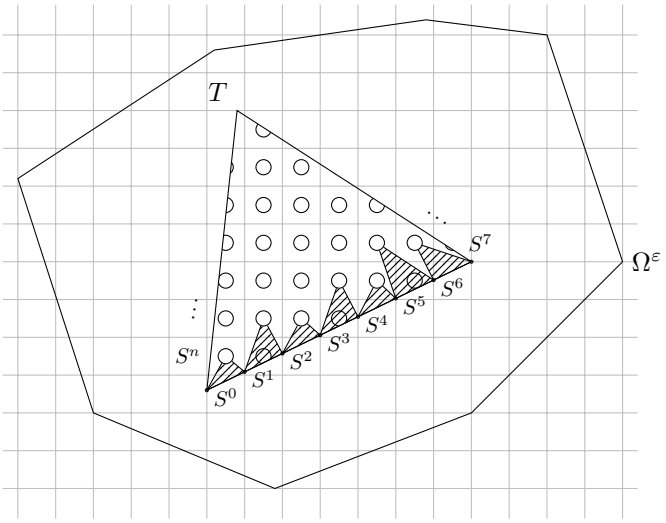

FIGURE 5. Partition of the boundary of T (bottom edge only, for clarity)

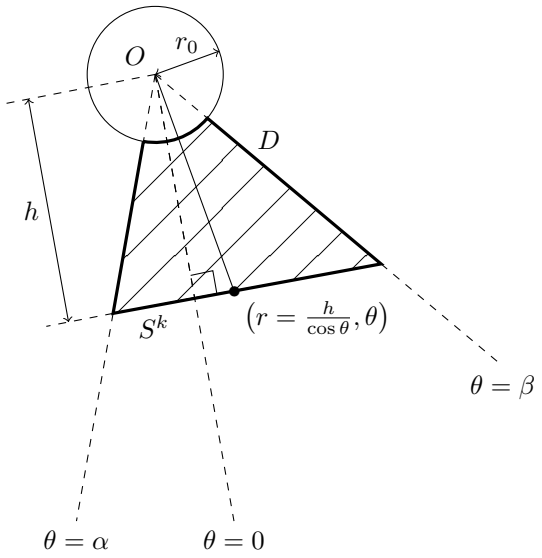

FIGURE 6. Local coordinates system associated to some S^k

r_0 centered at a point O and a "sector" D (see Fig. 6) which is bounded by two lines intersecting at O, by S itself and by a portion of the circle centered at O.

Let us fix a segment S as above and introduce properly shifted and rotated polar coordinates (r, θ) such that $r = 0$ corresponds to the disc center O and $\theta = 0$ corresponds to the direction normal to S, cf. Fig. 6. The segment S is parameterized in these coordinates as

$$\theta \in [\alpha, \beta] \mapsto X_\theta := \begin{pmatrix} r_\theta \\ \theta \end{pmatrix} \text{ with } r_\theta = \frac{h}{\cos\theta},$$

where h is the minimal distance from point O to the line containing S and $\alpha < 0 < \beta$. A simple geometrical calculation yields

$$|dX_\theta| = \frac{h}{\cos^2\theta} d\theta\,,$$

so that

$$\int_S v^2 = \int_\alpha^\beta v^2(r_\theta,\theta)\frac{h}{\cos^2\theta}d\theta\,,$$

where we write v as a function of polar coordinates (r,θ). Since v vanishes in the holes, we have $v(r_0,\theta)=0$ and

$$\begin{aligned}\int_S v^2 &= \int_\alpha^\beta \left(\int_{r_0}^{r_\theta} \frac{\partial v}{\partial r}(r,\theta)dr\right)^2 \frac{h}{\cos^2\theta}d\theta\\ &\le \int_\alpha^\beta \left(\int_{r_0}^{r_\theta} |\nabla v|^2(r,\theta)dr\right)(r_\theta - r_0)\frac{r_\theta^2}{h}d\theta\\ &\le \left(\max_{\theta\in[\alpha,\beta]}\frac{(r_\theta-r_0)r_\theta^2}{hr_0}\right)\int_\alpha^\beta\int_{r_0}^{r_\theta}|\nabla v|^2(r,\theta)r\,dr\,d\theta \le C\varepsilon\int_D|\nabla v|^2\,,\end{aligned}$$

with some constant $C>0$. Indeed, under our geometrical assumptions we have $h \ge r_0 \ge c_1\varepsilon$, $r_\theta \le c_2\varepsilon$ so that $\frac{(r_\theta-r_0)r_\theta^2}{hr_0} \le \frac{c_2^3}{c_1^2}\varepsilon$. Now, summing up over all the segments composing ∂T and noting that the sector D corresponding to such a segment S is inside the cell T and, moreover, for any two segments S, S' the corresponding sectors D, D' do not intersect, yields (46). □

Lemma 4.5 (Poincaré inequality on a perforated mesh cell)**.** *Suppose $H \ge \gamma\varepsilon$ with γ from Lemma 4.4. Then, for any $T \in \mathcal{T}_H$ and any $v \in H^1(T)^2$ vanishing on $B^\varepsilon \cap T$*

$$\|v\|_{L^2(T)} \le \varepsilon\, C\, |v|_{H^1(T)} \tag{47}$$

holds with some positive constant C independent of ε and H.

Proof. Applying a Poincaré inequality on the reference cell Y with the hole B and then rescaling to the cells of size ε gives

$$\|v\|_{L^2(Y_k)} \le \varepsilon\, C\, |v|_{H^1(Y_k)}$$

for any perforated cell Y_k, $k\in\mathbb{Z}^2$ and any $v \in H^1(Y_k)^2$ vanishing on B_k. Let $\mathcal{I}(T)\subset\mathbb{Z}^2$ be the set of indexes corresponding to the cells inside T and assume that the boundary of T is composed of m edges $E_1,\dots,E_m$. One can then introduce m rectangles $\Pi_1,\dots,\Pi_m$, each Π_i with base E_i and of width (in the direction perpendicular to E_i) $\le c\varepsilon$ with some H-independent constant c, so that

$$T \subset \cup_{k\in\mathcal{I}(T)} Y_k \cup \Pi_1 \cup \dots \cup \Pi_m\,,.$$

We can also safely assume that every point in T is covered by at most 3 subsets on the right-hand side of the inclusion above, i.e. at most by a cell Y_k and by two rectangles Π_i.

Let us introduce the Cartesian coordinates (ξ,η) on rectangle Π_i so that $\eta=0$, $\xi\in[0,|E_i|]$ corresponds to E_i and the coordinate η varies from 0 to some $h_i \le c\varepsilon$ on Π_i. Assuming that v is extended from $\Pi_i\cap T$ to the whole of Π_i so that the H_1 norm of v over Π_i remains bounded via that over $\Pi_i\cap T$, we calculate

$$\|v\|^2_{L^2(\Pi_i)} = \int_0^{|E_i|}\int_0^{h_i} v^2(\xi,\eta)d\eta d\xi$$

$$= h_i \int_0^{|E_i|} v^2(\xi,0)d\xi + \int_0^{|E_i|}\int_0^{h_i}\int_0^{\eta} 2v(\xi,s)\partial_\eta v(\xi,s)dsd\eta d\xi$$
$$\leq c\varepsilon\|v\|^2_{L^2(E_i)} + \frac{1}{2}\|v\|^2_{L^2(\Pi_i)} + C\varepsilon^2|v|^2_{H^1(\Pi_i)}\,.$$

Thus,

$$\|v\|^2_{L^2(\Pi_i\cap T)} \leq C(\varepsilon\|v\|^2_{L^2(E_i)} + \varepsilon^2|v|_{H^1(\Pi_i\cap T)})\,.$$

Summing over all the cells Y_k, $k\in\mathcal{I}(T)$ and all the rectangles Π_i and reminding that each point of T is covered by at most 3 such sets, gives

$$\|v\|^2_{L^2(T)} \leq C(\varepsilon\|v\|^2_{L^2(\partial T)} + \varepsilon^2|v|_{H^1(T)})\,,$$

which entails (47) thanks to Lemma 4.4. □

Lemma 4.6 (Poincaré inequality in H^1 - broken spaces)**.** *For any $v\in V_H^{ext}$*

$$\|v\|_{L^2(\Omega^\varepsilon)} \leq \varepsilon\, C|v|_{H^1(\Omega^\varepsilon)} \tag{48}$$

holds with some positive constant C indepdendent of ε.

Proof. We distinguish two cases: $H\geq\gamma\varepsilon$ with γ from Lemma 4.4 and $H<\gamma\varepsilon$. In the first case, the current lemma is a simple corollary of the previous one obtained by summing (47) over all the mesh cells. We thus assume from now on $H<\gamma\varepsilon$. Borrowing from [5] the idea of using an embedding theorem for BV spaces (the functions of bounded variation), we can write on each cell Y_k, $k\in\mathbb{Z}^2$ (of size ε, with the perforation B_k inside) and any $v\in V_H^{ext}$ extended by 0 outside Ω

$$\|v\|_{L^2(Y_k)} \leq C\,\mathrm{TV}_{Y_k}(v) := C \sup_{\varphi\in C^1_C(Y_k),|\varphi|\leq 1 \text{ on } Y_k} \int_{Y_k} v\,\mathrm{div}\,\varphi\,. \tag{49}$$

We have applied here Theorem 2 from [5], the proof of which can be found in [2, Chapter 3].[1] Note that we can use the semi-norm TV_{Y_k} of the BV space since v vanishes on the perforation B_k. The constant C is in principle domain dependent but it can be considered ε-independent in our case. Indeed, the inequality above is invariant under scaling $x\mapsto(x-x_k)/\varepsilon$ so that the value of C can be taken as that on the reference cell Y with its reference perforation B.

Integration by parts and the Cauchy-Schwarz inequality give for any $\varphi\in C^1_C(Y_k)$ such that $|\varphi|\leq 1$ on Y_k

$$\left|\int_{Y_k} v\,\mathrm{div}\,\varphi\right| = \left|-\int_{Y_k\setminus\mathcal{E}_H}\nabla v\cdot\varphi + \sum_{E\in\mathcal{E}_H}\int_{Y_k\cap E}[[v]]n\cdot\varphi\right|$$
$$\leq \varepsilon|v|_{H^1(Y_k)} + \left(\sum_{E\in\mathcal{E}_H}\|[[v]]\|^2_{L^2(Y_k\cap E)}\right)^{\frac12}\left(\sum_{E\in\mathcal{E}_H}|Y_k\cap E|\right)^{\frac12}$$
$$\leq \varepsilon|v|_{H^1(Y_k)} + C\frac{\varepsilon}{\sqrt{H}}\left(\sum_{E\in\mathcal{E}_H}\|[[v]]\|^2_{L^2(Y_k\cap E)}\right)^{\frac12}.$$

[1] We recall that the ambient dimension is assumed equal to 2 in this paper. Were we interested in the case of a perforated domain in $\mathbb{R}^d$ with $d>2$, we would have the norm of $L^{d/(d-1)}$ rather than L^2 in the left-hand side of (49). A proof of (48) could be then performed by first applying (49) to $|v|^\alpha$ with $\alpha = 2\frac{d-1}{d}$ rather than to v.

Indeed, the number of mesh edges intersecting Y_k is of the order of $\frac{\varepsilon^2}{H^2}$ and the length of each edge is smaller than H so that $\sum_{E\in\mathcal{E}_H}|Y_k\cap E|\leq C\frac{\varepsilon^2}{H}$. Taking the supremum over φ gives

$$\|v\|^2_{L^2(Y_k)}\leq C\left(\varepsilon^2|v|^2_{H^1(Y_k)}+\frac{\varepsilon^2}{H}\sum_{E\in\mathcal{E}_H}\|[[v]]\|^2_{L^2(Y_k\cap E)}\right).$$

Summing this over all the cells Y_k gives

$$\|v\|^2_{L^2(\Omega)}\leq C\left(\varepsilon^2|v|^2_{H^1(\Omega)}+\frac{\varepsilon^2}{H}\sum_{E\in\mathcal{E}_H}\|[[v]]\|^2_{L^2(Y_k)}\right).$$

By the trace inequality $\|[[v]]\|^2_{L^2(Y_k)}\leq CH|v|^2_{H^1(\omega_E)}$, this entails the desired result

$$\|v\|^2_{L^2(\Omega)}\leq C\varepsilon^2\left(|v|^2_{H^1(\Omega)}+\sum_{E\in\mathcal{E}_H}|v|^2_{H^1(\omega_E)}\right)\leq C\varepsilon^2|v|^2_{H^1(\Omega)}.$$

□

The three preceding lemmas could be established under more general geometrical assumptions than the periodic placement of the perforations. For example, a bound similar to that of Lemma 4.5 can be found in [34, Lemma A.1] in the case of randomly distributed perforations that are at a distance of order ε from one another. On the other hand, the proof of the following lemma uses extensively the results and notations on homogenization from Section 3, so that the periodicity assumption is essential there. This lemma will be the principal ingredient of the proof of Theorem 2.7.

Lemma 4.7. *Let u,p be the solution to the Stokes system (1)–(3) and set $p=p^*+p'$ where p^* is the solution to the Darcy problem (27)–(28). Under the same assumptions as those of Theorem 2.7 with γ from Lemma 4.4, we have, for any $v\in Z_H^{ext}:=\{v\in V_H^{ext}:\operatorname{div}v|_T=0\ \forall T\in\mathcal{T}_H\}$*

$$\left|\sum_{T\in\mathcal{T}_H}\int_{\partial T\cap\Omega^\varepsilon}((\nabla u)\,n-p'n)\cdot v\right| \leq C\varepsilon\left(\sqrt{\varepsilon}+\sqrt{\frac{\varepsilon}{H}}\right)|v|_{H^1(\Omega^\varepsilon)}\,\|f-\nabla p^*\|_{H^2(\Omega)\cap C^1(\bar\Omega)}, \quad (50)$$

where the constant C is independent of H, ε, f and v.

Proof. Using the divergence theorem on any $T\in\mathcal{T}_H$ and reminding (40) and $\operatorname{div}v=0$ on T, we observe that

$$\begin{aligned}
&\sum_{T\in\mathcal{T}_H}\int_{\partial T\cap\Omega^\varepsilon}((\nabla u)\,n-p'n)\cdot v\\
&=\sum_{T\in\mathcal{T}_H}\int_{\Omega^\varepsilon\cap T}\nabla u:\nabla v-\int_{\Omega_\varepsilon\cap T}(f-\nabla p^*)\cdot v\\
&=\sum_{T\in\mathcal{T}_H}\left[\int_{\Omega^\varepsilon\cap T}(\nabla u-\nabla\tilde u^*):\nabla v+\int_{\Omega^\varepsilon\cap T}(\nabla\tilde u^*-(\tilde p^{\varepsilon,1}-p^*)\,I):\nabla v\right.\\
&\qquad\left.-\int_{\Omega^\varepsilon\cap T}(f-\nabla p^*)\cdot v\right]
\end{aligned}$$

$$= \sum_{T\in\mathcal{T}_H}\int_{\Omega^\varepsilon\cap T}(\nabla u-\nabla\tilde{u}^*):\nabla v+\sum_{T\in\mathcal{T}_H}\int_{\Omega_\varepsilon\cap\partial T}\left((\nabla\tilde{u}^*)\,n-\left(\tilde{p}^{\varepsilon,1}-p^*\right)n\right)\cdot v$$
$$-\sum_{T\in\mathcal{T}_H}\int_{\Omega^\varepsilon\cap T}(f+\Delta\tilde{u}^*-\nabla\tilde{p}^{\varepsilon,1})\cdot v\,. \tag{51}$$

The first term in the sum above can be bounded by

$$C\varepsilon\sqrt{\varepsilon}\|f-\nabla p^*\|_{H^2(\Omega)\cap C^1(\bar{\Omega})}|v|_{H^1(\Omega^\varepsilon)}\,,$$

using the homogenization estimate (31). We turn now to the second term in (51).

Using Lemmas 4.1 and 4.4 and the fact that $\tilde{w}_i$, $\tilde{\pi}_i$ and $\nabla\tilde{w}_i$ are uniformly bounded, we have for any $T\in\mathcal{T}_H$

$$\left|\int_{\Omega^\varepsilon\cap\partial T}((\nabla\tilde{u}^*)n-(\tilde{p}^{\varepsilon,1}-p^*)n)\cdot v\right|$$
$$=\left|\int_{\partial T\cap\Omega^\varepsilon}\left[\varepsilon(\nabla\tilde{w}_i)_\varepsilon n(f_i-\partial_i p^*)+\varepsilon^2(\tilde{w}_i)_\varepsilon\cdot\nabla(f_i-\partial_i p^*)n-\varepsilon(\tilde{\pi}_i)_\varepsilon(f_i-\partial_i p^*)\right]\cdot v\right|$$
$$\le C\|v\|_{L^2(\partial T)}[\varepsilon\|f-\nabla p^*\|_{L^2(\partial T)}+\varepsilon^2\|\nabla(f-\nabla p^*)\|_{L^2(\partial T)}]$$
$$\le C\varepsilon\sqrt{\frac{\varepsilon}{H}}|v|_{H^1(T)}\,\|f-\nabla p^*\|_{H^2(T)}\,.$$

Now, summing up over all the cells and using the discrete Cauchy-Schwarz inequality yields

$$\left|\sum_{T\in\mathcal{T}_H}\int_{\Omega^\varepsilon\cap\partial T}((\nabla u^*)n-(\tilde{p}^{\varepsilon,1}-p^*)n)\cdot v\right|\le C\varepsilon\sqrt{\frac{\varepsilon}{H}}\,|v|_{H^1(\Omega^\varepsilon)}\,\|f-\nabla p^*\|_{H^2(\Omega)}.$$

To bound the third term in (51), we recall the definition of F_ε (41) and observe that

$$f+\Delta\tilde{u}^*-\nabla\tilde{p}^{\varepsilon,1}=F_\varepsilon\,.$$

Thus, using the estimate of F_ε and the Poincaré inequality from Lemma 4.6,

$$\left|\sum_{T\in\mathcal{T}_H}\int_{\Omega^\varepsilon\cap T}(f+\Delta\tilde{u}^*-\nabla\tilde{p}^{\varepsilon,1}):v\right|\le C\varepsilon\sqrt{\varepsilon}\|f-\nabla p^*\|_{H^2(\Omega)\cap C^1(\bar{\Omega})}\,|v|_{H^1(\Omega^\varepsilon)}\,.$$

Summing up the bounds for all the three terms in (51) yields (50). □

5. **Proof of Theorem 2.7.** We note first of all that error estimate (20) is trivial if H is of order ε or smaller. Indeed, if $H\le\gamma\varepsilon$, then (20) is reduced to

$$|u-u_H|_{H^1(\Omega)}+\varepsilon\|p-p_H\|_{L^2(\Omega)}\le C\varepsilon(\|f-\nabla p^*\|_{H^2(\Omega)\cap C^1(\bar{\Omega})}+|p^*|_{H^2(\Omega)})\,, \tag{52}$$

with a constant C depending on γ. But we have, in fact for any ε and H,

$$|u|_{H^1(\Omega)}+\varepsilon\|p\|_{L^2(\Omega)}\le C\varepsilon\|f\|_{L^2(\Omega)}\,,$$
$$|u_H|_{H^1(\Omega)}+\varepsilon\|p_H\|_{L^2(\Omega)}\le C\varepsilon\|f\|_{L^2(\Omega)}\,.$$

These estimates for the velocity are easily obtained from the Poincaré inequality on the perforated domain Ω^ε which is valid even for the broken H^1 Sobolev space, as proven in Lemma 4.6. As for the pressure, these are the standard bounds for the solutions of saddle-point problems since the inf-sup property holds with a constant of order ε both on continuous and discrete levels, cf. Lemmas 3.2 and 2.5. This clearly entails (52) and consequently (20) if $H<\gamma\varepsilon$.

We thus assume from now on $H \geq \gamma\varepsilon$ with γ from Lemma 4.4 and use without further notice Lemmas 4.4, 4.5, 4.7 from the previous section. Our error estimate is essentially based on a Strang lemma (e.g. [6, Lemma 10.1.7])

$$|u - u_H|_{H^1} \leq \inf_{v \in Z_H} |u - v|_{H^1} + \sup_{v \in Z_H \setminus \{0\}} \frac{|a(u - u_H, v)|}{|v|_{H^1}}\,, \tag{53}$$

where u is the solution to (1)–(3) and u_H is the solution to (15).

To bound the first term in (53), we recall that u is the solution to problem (1)–(3) and introduce

$$v_H(x) = \sum_{E \in \mathcal{E}_H} \sum_{i=1}^{3} \left(\int_E u \cdot \psi_{E,i} \right) \Phi_{E,i}(x),$$
$$q_H(x) = \sum_{E \in \mathcal{E}_H} \sum_{i=1}^{3} \left(\int_E u \cdot \psi_{E,i} \right) \pi_{E,i}(x)\,,$$

with $\Phi_{E,i}$ and $\pi_{E,i}$ defined in Lemma 2.4 with the weights ω_{E_i} chosen as in (19). Observe, for all edges $E \in \mathcal{E}_H$ and all cells $T \in \mathcal{T}_H$, that

$$\begin{aligned}
\int_E v_H &= \int_E u\,,\\
\int_E \psi_E v_H \cdot n_E &= \int_E \psi_E u \cdot n_E\,,\\
(\nabla v_H)\, n - q_H n &= a + b\, n_E \psi_E \quad \text{on (each side of) } E\\
&\qquad \text{with } a \in \mathbb{R}^2, b \in \mathbb{R},\\
-\Delta v_H + \nabla q_H &= 0 \text{ on } T \cap \Omega_\varepsilon\,.
\end{aligned} \tag{54}$$

By construction, $v_H \in V_H$. Moreover, it is easy to see that $v_H \in Z_H$. Indeed, for any $T \in T_H$ we have $\operatorname{div} v_H = c_T$ on $T \setminus B^\varepsilon$ with some constant c_T and

$$c_T |T \setminus B^\varepsilon| = \int_T \operatorname{div} v_H = \int_{\partial T} n \cdot v_H = \int_{\partial T} n \cdot u = 0\,,$$

so that $c_T = 0$.

We also have, setting $p = p^* + p'$, as in Lemma 4.7

$$\begin{aligned}
|u - v_H|^2_{H^1(\Omega^\varepsilon)} &= \sum_{T \in \mathcal{T}_H} \int_{\Omega^\varepsilon \cap T} \nabla(u - v_H) : \nabla(u - v_H)\\
&\quad - \sum_{T \in \mathcal{T}_H} \int_{\Omega^\varepsilon \cap T} (p' - q_H) \operatorname{div}(u - v_H)\\
&= \sum_{T \in \mathcal{T}_H} \int_{\Omega^\varepsilon \cap T} (-\Delta(u - v_H) + \nabla(p' - q_H)) \cdot (u - v_H)\\
&\quad + \sum_{T \in \mathcal{T}_H} \int_{\partial T \cap \Omega^\varepsilon} (u - v_H) \cdot ((\nabla u) n - p' n)\\
&\quad - \sum_{T \in \mathcal{T}_H} \int_{\partial T \cap \Omega_\varepsilon} (u - v_H) \cdot ((\nabla v_H) n - q_H n)\,.
\end{aligned} \tag{55}$$

We now successively bound the three terms of the right-hand side of (55).

- For the first term, we observe that $\int_E s\,(u-v_H)\cdot n_E = 0$ for any $E \in \mathcal{E}_H$ and for any polynomial $s \in \mathbb{P}_1(E)$. It means that $\forall T \in \mathcal{T}_H$ and $\forall a \in \mathbb{R}^2$

$$\int_T a\cdot(u-v_H) = \int_T \nabla(a\cdot x)\cdot(u-v_H) = \int_{\partial T}(a\cdot x)n\cdot(u-v_H) = 0\,,$$

since $\operatorname{div}(u-v_H)=0$. In particular,

$$\sum_{T\in\mathcal{T}_H}\int_{\Omega^\varepsilon\cap T}\Pi_H(f-\nabla p^*)\cdot(u-v_H) = 0\,,$$

where Π_H is the projection on piecewise constant functions, as in Lemma 4.2. Recalling the last line in (54) and using (45) and (48), we get

$$\begin{aligned}
&\sum_{T\in\mathcal{T}_H}\int_{\Omega^\varepsilon\cap T}(-\Delta(u-v_H)+\nabla(p'-q_H))\cdot(u-v_H)\\
&\quad= \sum_{T\in\mathcal{T}_H}\int_{\Omega^\varepsilon\cap T}(f-\nabla p^*-\Pi_H(f-\nabla p^*))\cdot(u-v_H)\\
&\quad\le \|(f-\nabla p^*)-\Pi_H(f-\nabla p^*)\|_{L^2(\Omega)}\,\|u-v_H\|_{L^2(\Omega^\varepsilon)}\\
&\quad\le C\varepsilon H|(f-\nabla p^*)|_{H^1(\Omega)}|u-v_H|_{H^1(\Omega^\varepsilon)}\,.
\end{aligned}$$

- The second term in (55) is bounded by

$$C\varepsilon\left(\sqrt{\varepsilon}+\sqrt{\frac{\varepsilon}{H}}\right)|u-v_H|_{H^1(\Omega^\varepsilon)}\,\|f-\nabla p^*\|_{H^2(\Omega)\cap C^1(\bar\Omega)}\,,$$

thanks to Lemma 4.7.
- The third term in (55) vanishes. Indeed, on each edge E, we know from (54) that $n\cdot\nabla v_H - q_H\,n = a + b\,n_E\psi_E$ with some constants $a\in\mathbb{R}^2$, $b\in\mathbb{R}$ and $\int_E(a+b\,n_E\psi_E)\cdot(u-v_H)=0$ by construction of $u-v_H$.

Collecting all these estimates, we deduce that

$$|u-v_H|_{H^1(\Omega^\varepsilon)} \le C\varepsilon\left(\sqrt{\varepsilon}+H+\sqrt{\frac{\varepsilon}{H}}\right)\|f-\nabla p^*\|_{H^2(\Omega)\cap C^1(\bar\Omega)}.$$

This concludes the estimate for the first term of (53).

We now turn to the nonconformity error, i.e. the second term in (53). Let $v\in Z_H$. We use (15) and $\operatorname{div} v = 0$ to compute

$$\begin{aligned}
&\int_{\Omega^\varepsilon}\nabla(u-u_H):\nabla v\\
&\quad= \sum_{T\in\mathcal{T}_H}\left(\int_{\Omega^\varepsilon\cap T}\nabla u:\nabla v - \int_{\Omega^\varepsilon\cap T}p'\operatorname{div} v\right) - \int_{\Omega^\varepsilon} f\cdot v\\
&\quad= \sum_{T\in\mathcal{T}_H}\int_{\partial T\cap\Omega^\varepsilon} v\cdot((\nabla u)n - p'n) - \sum_{T\in\mathcal{T}_H}\int_{\Omega_\varepsilon\cap T}(f+\Delta u-\nabla p')\cdot v\\
&\quad= \sum_{T\in\mathcal{T}_H}\int_{\partial T\cap\Omega^\varepsilon} v\cdot((\nabla u)n - p'n) - \sum_{T\in\mathcal{T}_H}\int_T \nabla p^*\cdot v\,.
\end{aligned}$$

The first term in the right-hand side above is bounded thanks to Lemma 4.7 by $C\varepsilon\left(\sqrt{\varepsilon}+\sqrt{\frac{\varepsilon}{H}}\right)\|f-\nabla p^*\|_{H^2(\Omega)\cap C^1(\bar\Omega)}\,|v|_{H^1}$. To bound the second term, we shall

use $I_H p^* \in H^1(\Omega)$ as constructed in Lemma 4.3. Observe that

$$\sum_{T\in\mathcal{T}_H} \int_T \nabla(I_H p^*)\cdot v = \sum_{E\in\mathcal{E}_H} \int_E I_H p^*\, n_E \cdot [[v]] = 0\,, \tag{56}$$

since $I_H p^*$ is a polynomial of degree ≤ 1 on each edge $E \in \mathcal{E}_H$. Thus, using Lemmas 4.3 and 4.6,

$$\begin{aligned}\left|\sum_{T\in\mathcal{T}_H} \int_T \nabla p^*\cdot v\right| &= \left|\sum_{T\in\mathcal{T}_H} \int_T \nabla(p^* - I_H p^*)\cdot v\right| \\ &\leq |p^* - I_H p^*|_{H^1(\Omega)} \|v\|_{L^2(\Omega)} \leq \varepsilon H |p^*|_{H^2(\Omega)} |v|_{H^1(\Omega)}\,. \end{aligned}\tag{57}$$

Finally,

$$\begin{aligned}&\sup_{v\in V_H\setminus\{0\}} \frac{|a(u-u_H,v)|}{|v|_{H^1}} \\ &\qquad \leq C\varepsilon\left[\left(\sqrt{\varepsilon}+\sqrt{\frac{\varepsilon}{H}}+H\right)\|f-\nabla p^*\|_{H^2(\Omega)\cap C^1(\bar\Omega)} + H|p^*|_{H^2(\Omega)}\right],\end{aligned}$$

which proves the estimate for $(u-u_H)$ in (20).

Remark 6. We have just seen that the nonconformity error has been treated with the help of the trick (56)–(57) which requires the jumps of the normal component of velocities in Z_H to be orthogonal to polynomials of degree 1 on any edge. This is exactly the motivation to introduce the weights CR_3 (19). This proof would not work with CR_2 weights, even if the MsFEM bubbles were added, as suggested in Remark 4.

We turn now to the error estimate for pressure. Using operators Π_H and I_H from Lemmas 4.2 and 4.3, we set $p_H^* = \Pi_H I_H p^* \in M_H$, i.e. the L^2-orthogonal projection of $I_H p^*$ on M_H. By interpolation estimates (45), (4.3) and homogenization bounds

$$\begin{aligned}\|p_H^* - p\|_{L^2(\Omega^\varepsilon)} &\leq \|\Pi_H(I_H p^* - p^*)\|_{L^2(\Omega)} + \|\Pi_H p^* - p^*\|_{L^2(\Omega)} + \|p^* - p\|_{L^2(\Omega^\varepsilon)} \\ &\leq \|I_H p^* - p^*\|_{L^2(\Omega)} + \|\Pi_H p^* - p^*\|_{L^2(\Omega)} + \|p^* - p\|_{L^2(\Omega^\varepsilon)} \\ &\leq C(H|p^*|_{H^1(\Omega)} + \sqrt{\varepsilon}\|f-\nabla p^*\|_{H^2(\Omega)\cap C^1(\bar\Omega)}).\end{aligned}\tag{58}$$

Now, in view of the inf-sup lemmas (2.5) and (3.2), there exists $v_H \in V_H$ such that for any $T \in \mathcal{T}_H$

$$\operatorname{div} v_H = p_H - p_H^* \text{ on } T\cap\Omega^\varepsilon \quad \text{and} \quad |v_H|_{H^1(\Omega)} \leq \frac{C}{\varepsilon}\|p_H - p_H^*\|_{L^2(\Omega^\varepsilon)}\,. \tag{59}$$

Integration by parts element by element yields

$$\begin{aligned}\|p_H - p_H^*\|^2_{L^2(\Omega^\varepsilon)} &= \int_{\Omega^\varepsilon} (p_H - p_H^*)\operatorname{div} v_H \\ &= -\int_{\Omega^\varepsilon} f\cdot v_H + \int_{\Omega^\varepsilon} \nabla u_H : \nabla v_H - \int_{\Omega^\varepsilon} p_H^* \operatorname{div} v_H \\ &= \int_{\Omega^\varepsilon} (\Delta u - \nabla(p^*+p'))\cdot v_H + \int_{\Omega^\varepsilon} \nabla u_H : \nabla v_H - \int_{\Omega^\varepsilon} p_H^* \operatorname{div} v_H \\ &= \int_{\Omega^\varepsilon} \nabla(u_H - u) : \nabla v_H + \int_{\Omega^\varepsilon} p' \operatorname{div} v_H + \sum_{T\in\mathcal{T}_H} \int_{\partial T\cap\Omega_\varepsilon} v_H\cdot((\nabla u)n - p'n) \\ &\qquad - \int_{\Omega^\varepsilon} \nabla(p^* - I_H p^*)\cdot v_H - \int_{\Omega^\varepsilon} \nabla I_H p^*\cdot v_H - \int_{\Omega^\varepsilon} p_H^* \operatorname{div} v_H\,.\end{aligned}$$

In fact, the last two terms above cancel each other. Indeed,

$$-\int_{\Omega^\varepsilon} \nabla I_H p^* \cdot v_H - \int_{\Omega^\varepsilon} p_H^* \operatorname{div} v_H = -\sum_{E\in\mathcal{E}_H} \int_E I_H p^* [[n\cdot v_H]] + \int_{\Omega^\varepsilon} (I-\Pi_H)(I_H p^*) \operatorname{div} v_H = 0\,.$$

This is zero since $[[n \cdot v_H]]$ is orthogonal to the polynomials of degree ≤ 1 on the edges and $\operatorname{div} v_H \in M_H$.

We can now apply the already proven upper bound for the velocity error $(u-u_H)$ in (20), Lemma 4.7, and bound (57) to conclude

$$\begin{aligned}\|p_H - p_H^*\|^2_{L^2(\Omega^\varepsilon)} &\leq C\varepsilon \left[\left(\sqrt{\varepsilon} + \sqrt{\frac{\varepsilon}{H}} + H\right) \|f - \nabla p^*\|_{H^2(\Omega)\cap C^1(\bar\Omega)} + H|p^*|_{H^2(\Omega)}\right] \|v_H\|_{H^1(\Omega)} \\ &\quad + \|p'\|_{L^2(\Omega^\varepsilon)} \|\operatorname{div} v_H\|_{L^2(\Omega)}\,.\end{aligned}$$

Recalling the properties of v_H (59) and the homogenization estimate (29) for $p' = p - p^*$, this entails

$$\|p_H - p_H^*\|_{L^2} \leq C\left[\left(\sqrt{\varepsilon} + \sqrt{\frac{\varepsilon}{H}} + H\right) \|f - \nabla p^*\|_{H^2(\Omega)\cap C^1(\bar\Omega)} + H|p^*|_{H^2(\Omega)}\right]\,,$$

which in combination with (58) gives the error estimate for pressure in (20) by the triangle inequality.

Remark 7. The MsFEM approach presented here can be extended to the 3D case, with some caveats. In order to keep a 3D analogue of (54), we should require then 5 weights $\omega_{E,i}$, cf. (19), to allow for arbitrary linear polynomials in the normal direction on every edge. The numerical analysis of Sections 4 and 5 would then be extended flawlessly from 2D to 3D.
Extending the homogenization error analysis of Section 3 is much less straightforward. Here, in 2D, the analysis is carried out for periodic, separated obstacles. Physically, this corresponds to a flow between vertical pillars, attached to the immobile wall at the bottom/top of a 3D domain that can be projected on the horizontal plane. In 3D, homogenization error estimates are available in [36], but they are obtained under the same geometrical assumptions as in 2D: one models a fluid flowing between isolated sphere-like obstacles, that are not connected between themselves or to anything else, but remain immobile. The physical relevance of such a model is debatable. Obstacles made of a connected, porous structure would be closer to the reality, cf. [1], but a quantitative homogenization error analysis in this case is not yet available.

6. Numerical results.

In this section we show some results of numerical computations, for both variants of our method, CR_2 and CR_3, cf. (18) and (19). All calculations are performed in `FreeFem++` [22], the scripts are available at the following address: https://github.com/gjankowiak/stokes_msfem.

6.1. Implementation details.

The Crouzeix-Raviart MsFEM as presented so far relies on the exact solutions of the local problems in the construction of the basis functions. In practice, these problems should be discretized on a mesh sufficiently

fine to resolve the geometry of obstacles. To avoid complex and ad-hoc grid generation methods when solving (1)–(3) in Ω^ϵ we replace it with the penalized problem, cf. [32]. To calculate both the basis functions and the reference solutions, we use the P1-P1 FEM on the uniform Cartesian grid $\mathcal{T}_h$ of step $h \ll H$. As is well known, this choice of velocity and pressure spaces requires some stabilization which weakens the condition $\nabla \cdot \vec{u} = 0$. The simplest way to achieve this is by perturbing the incompressibility constraint with a pressure Laplacian term, see [7] and [32]. Note that the error introduced by the penalized problem (of order $\sqrt{h}$) is larger than that of the $P1 - P1$ FEM stabilization. A more accurate discretization of local problems, on fine meshes resolving the obstacles, is presented in [18, 19].

The reference solution is calculated on the global mesh of the same size as that for the MsFEM basis functions.

6.2. **Test case with periodic holes.** For our first test case we choose $\Omega = (0,1)^2$ and B^ε as the set of discs of radius $\varepsilon/4$ placed periodically on a regular grid of period $\varepsilon = \frac{1}{135}$. We solve Stokes equations (1)–(3) on $\Omega^\varepsilon = \Omega \setminus B^\varepsilon$ with $f = 100 \begin{pmatrix} -(x_2 - 1/2) \\ x_1 - 1/2 \end{pmatrix}$. The fine regular Cartesian mesh with $h = \frac{1}{2160}$ is used to compute both the reference solution and the MsFEM basis functions. Numerical results in Fig. 7 clearly confirm the superiority of the CR3 variant over the CR2 one.

A (coarse) mesh refinement study is reported in Fig. 8. The error curves for the CR_3 velocity approximation are somewhat difficult to interpret. Qualitatively, they confirm the complex structure of the error, as suggested by the theoretical estimate (20). The error comes from two principal sources: a standard finite element approximation of the homogenized pressure (the error of order H in the H^1 norm), and the spurious boundary layers in the MsFEM basis functions near the edges of the mesh (the error of order $\sqrt{\varepsilon/H}$). At the range of H to ε ratios that we were able to investigate, neither of these factors seems to prevail over the other (similar findings are reported in [30] in the case of diffusion equation on perforated domains). Moreover, there should be more subtle sources of the error that are not revealed by our theoretical analysis. For instance, the approximation seems to improve significantly when the size of coarse mesh cells H is a multiple of the period of the obstacle structure ε. This phenomenon is much less noticeable for CR_2, presumably because of the general poor approximation it provides (as expected, CR_3 variant of the method produces a much more accurate solution than CR_2 one).

The error curves for $p - p_H$ (with p_H being the piecewise constant approximation to the exact pressure p) are qualitatively better than the theoretical bound (20). Apart from the piecewise approximation p_H we also report on an "oscillating" reconstruction $p_H + \pi_H(u_H)$ as suggested by (11), i.e. reusing the local pressure contributions $\pi_{E,i}$ associated to the velocity basis functions $\Phi_{E,i}$. Somewhat surprisingly, this does not improves the accuracy of the approximation, except for our finest mesh with $H = \varepsilon$.

6.3. **Channel flow.** We turn now to a more realistic test case: a flow in a rectangle $\Omega = (0,2) \times (0,1)$ with around 2500 obstacles B^ε of size 10^{-3} randomly distributed inside the domain, with a parabolic velocity profile prescribed on the left and right sides of Ω. We solve thus (1)–(2)–(17) with $f = 0$ and the boundary conditions $u = x_2(1-x_2)e_1$ on $\partial\Omega$. The adaptation of our method in view of non-homogeneous boundary conditions is presented in Remark 3.

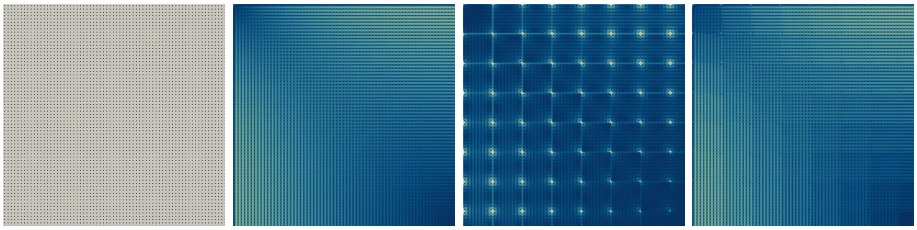

FIGURE 7. Test case of Section 6.2, cropped to the upper left quadrant. From left to right: fluid domain Ω^ε, with obstacles in black; the reference solution on the 2160×2160 grid; the CR_2 MsFEM solution on 15×15 grid; same with CR_3. On the last 3 plots, the velocity magnitude is represented using the same color code everywhere.

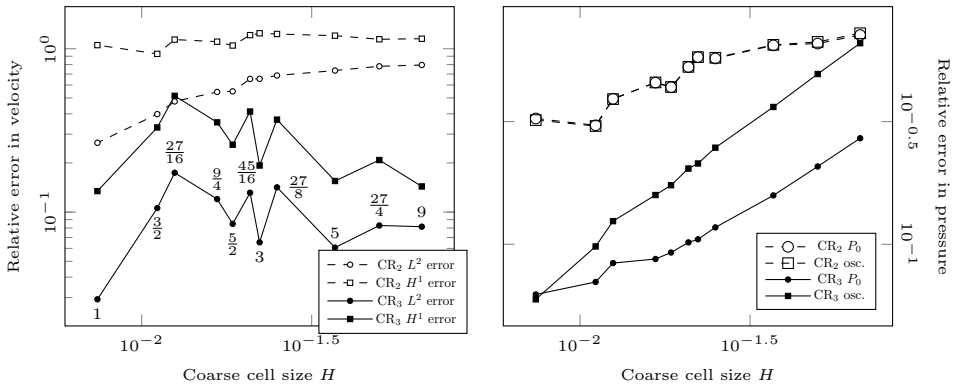

FIGURE 8. Test case of Section 6.2. Left: the relative error in velocity $u - u_H$ in L^2 and H^1 norms. Right: the relative error in pressure computed either as $p - p_H$ (denoted P_0) or as $p - p_H - \pi_H(u_H)$ (denoted osc.). The mesh size H varies from $\frac{1}{15}$ down to $\frac{1}{135}$ with $\varepsilon = \frac{1}{135}$. The fractions indicate the ratio $\frac{135}{H^{-1}}$, where we recall that 135 and H^{-1} are the number of obstacles and coarse cells along a given axis, respectively. When this ratio is an integer, the approximation error improves.

The reference solution and MsFEM CR_2 and CR_3 solutions (namely the u_1 velocity component) are reported in Fig. 9. We observe that the CR_3 variant captures the essential features of the solution even on a very coarse 8×4 mesh, while the solution produced by the CR_2 variant is completely wrong. The errors on a succession of coarse meshes are reported at Fig. 10. As for the pressure, we can note that its "oscillating" reconstruction $p_H + \pi_H(u_H)$ is systematically more accurate than p_H alone (contrary to the previous test case), but a significant improvement is observed only on the coarsest meshes.

6.4. **Cavity driven flow.** Finally, still in a rectangle $\Omega = (0, 2) \times (0, 1)$ with 100 randomly distributed obstacles of size about 10^{-3}, we solve (1)–(2)–(17) with $f = 0$ and $u = e_1$ on the top boundary and $u = 0$ on the rest of $\partial\Omega$. Some solutions are

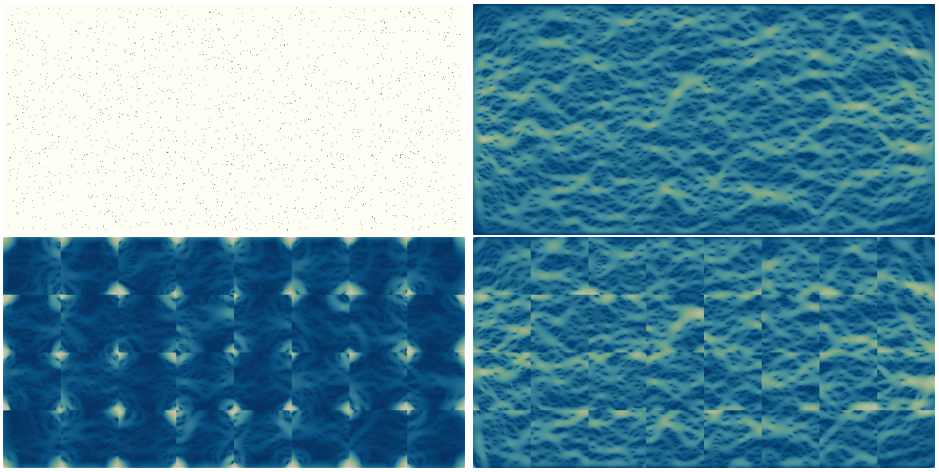

FIGURE 9. Test case of Section 6.3: channel flow. Top left : fluid domain Ω^ε, with obstacles in black. Top right: the reference solution on the 2160×1080 grid. Bottom: the MsFEM solution on 8×4 grid; CR_2 on the left, CR_3 on the right. The velocity magnitude is represented on the contour plots.

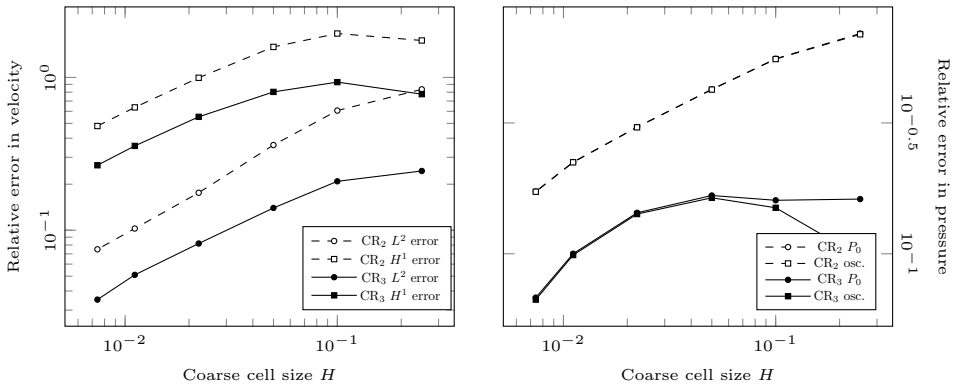

FIGURE 10. Test case of Section 6.3. Left: the relative error in velocity $u - u_H$ in L^2 and H^1 norms. Right: the relative error in pressure computed either as $p - p_H$ (denoted P_0) or as $p - p_H - \pi_H(u_H)$ (denoted osc.). The mesh size H varies from $\frac{1}{4}$ down to $\frac{1}{135}$ with $\varepsilon = \frac{1}{135}$.

represented at Fig. 11 and the errors are reported at Fig. 12. As for the pressure, the improvement produced by the "oscillating" reconstruction $p_H + \pi_H(u_H)$ over p_H alone is now observed on all the meshes. Summing up all the observation with respect to this issue, we conclude that putting some extra effort into the reconstruction of the oscillating part $\pi_H(u_H)$ is beneficial (sometimes significantly) in the majority of cases.

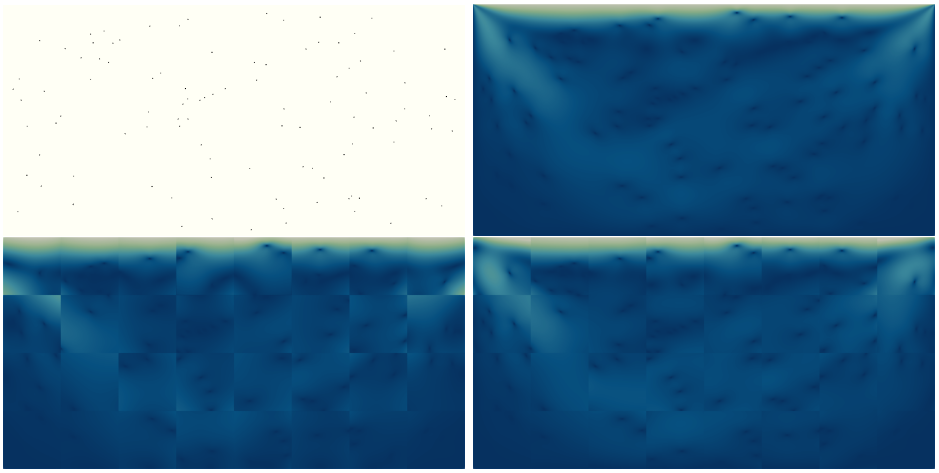

FIGURE 11. Test case of Section 6.4: cavity driven flow. Top left : fluid domain Ω^ε, with obstacles in black. Top right: the reference solution on the 2160×1080 grid. Bottom: the MsFEM solution on 8×4 grid; CR_2 on the left, CR_3 on the right. The velocity magnitude is represented on the contour plots.

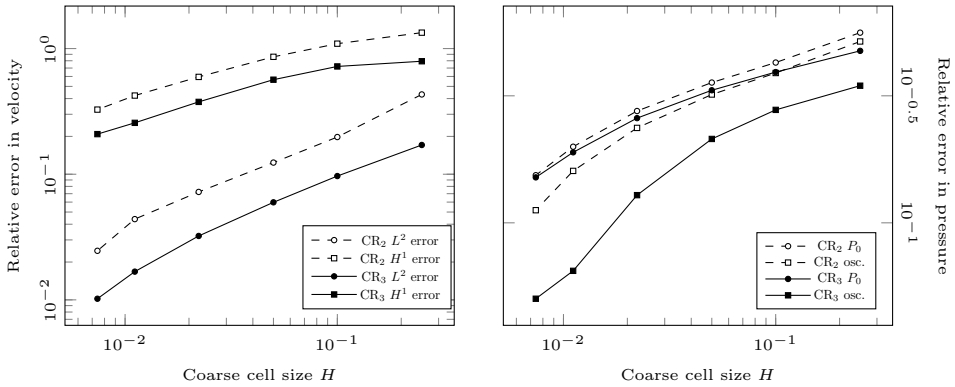

FIGURE 12. Test case of Section 6.4. Left: the relative error in velocity $u - u_H$ in L^2 and H^1 norms. Right: the relative error in pressure computed either as $p - p_H$ (denoted P_0) or as $p - p_H - \pi_H(u_H)$ (denoted osc.). The mesh size H varies from $\frac{1}{4}$ down to $\frac{1}{135}$ with $\varepsilon = \frac{1}{135}$.

Acknowledgments. The first author acknowledges the financial support of Région Bourgogne-Franche-Comté that has permitted to start the work on this article during his stay at Besançon. The second author is grateful to Prof. Grégoire Allaire for his interest in this work and for several enlightening discussions.

REFERENCES

[1] G. Allaire, Homogenization of the Stokes flow in a connected porous medium, *Asymptotic Anal.*, **2** (1989), 203-222.

[2] L. Ambrosio, N. Fusco and D. Pallara, *Functions of Bounded Variation and Free Discontinuity Problems*, Oxford Mathematical Monographs, The Clarendon Press, Oxford University Press, New York, 2000.
[3] M. Bebendorf, A note on the Poincaré inequality for convex domains, *Zeitschrift für Analysis und ihre Anwendungen*, **22** (2003), 751-756.
[4] L. Beirão da Veiga, F. Brezzi, A. Cangiani, G. Manzini, L. D. Marini and A. Russo, Basic principles of virtual element methods, *Math. Models Methods Appl. Sci.*, **23** (2013), 199-214.
[5] M. Bessemoulin-Chatard, C. Chainais-Hillairet and F. Filbet, On discrete functional inequalities for some finite volume schemes, *IMA J. Numer. Anal.*, **35** (2015), 1125-1149.
[6] S. C. Brenner and L. R. Scott, *The Mathematical Theory of Finite Element Methods*, vol. 15 of Texts in Applied Mathematics, 3rd edition, Springer, New York, 2008.
[7] F. Brezzi and J. Pitkaranta, On the stabilization of finite element approximations of the stokes problem, *Efficient Solutions of Elliptic Systems, Notes on Numerical Fluid Mechanics*, **10** (1984), 11-19.
[8] D. Brown, Y. Efendiev and V. Hoang, An efficient hierarchical multiscale finite element method for Stokes equations in slowly varying media, *SIAM MMS*, **11** (2013), 30-58.
[9] D. Brown, Y. Efendiev, G. Li, P. Popov and V. Savatorova, Multiscale modeling of high contrast Brinkman equations with applications to deformable porous media, in *Poromechanics V*, **235** (2013), 1991-1996.
[10] J. Chu, Y. Efendiev, V. Ginting and T. Hou, Flow based oversampling technique for multiscale finite element methods, *Advances in Water Resources*, **31** (2008), 599-608.
[11] M. Crouzeix and P. A. Raviart, Conforming and nonconforming finite element methods for solving the stationary Stokes equations I, *RAIRO*, **7** (1973), 33-75.
[12] P. Degond, A. Lozinski, B. P. Muljadi and J. Narski, Crouzeix-Raviart MsFEM with Bubble Functions for Diffusion and Advection-Diffusion in Perforated Media, *Comm. Comp. Phys.,* **17** (2015), 887-907.
[13] M. Dorobantu and B. Engquist, Wavelet-based numerical homogenization, *SIAM J. Numer. Anal.*, **35** (1998), 540-559.
[14] W. E and B. Engquist, The heterogeneous multi-scale methods, *Comm. Math. Sci.*, **1** (2003), 87-132.
[15] Y. Efendiev, J. Galvis, G. Li and M. Presho, Generalized multiscale finite element methods. oversampling strategies, *Int. J. Multiscale Comp. Eng.*, **12** (2014), 465-484.
[16] Y. Efendiev and T. Y. Hou, *Multiscale Finite Element Method, Theory and Applications. Surveys and Tutorials in the Applied Mathematical Sciences*, Springer, New York, 2009.
[17] A. Ern and J.-L. Guermond, *Theory and Practice of Finite Elements*, vol. 159 of Applied Mathematical Sciences, Springer-Verlag, New York, 2004.
[18] Q. Feng, *Development of a Multiscale Finite Element Method for Incompressible Flows in Heterogeneous Media*, PhD Thesis, Université Paris Saclay (COmUE), 2019, `https://tel.archives-ouvertes.fr/tel-02325512`.
[19] Q. Feng, G. Allaire and P. Omnes, Enriched nonconforming multiscale finite element method for Stokes flows in heterogeneous media based on high-order weighting functions, *Multiscale Modeling & Simulation*, **20** (2022), 462-492.
[20] V. Girault and P.-A. Raviart, *Finite Element Methods for Navier-Stokes Equations*, Theory and algorithms, vol. 5 of Springer Series in Computational Mathematics, Springer-Verlag, Berlin, 1986.
[21] P. Grisvard, *Elliptic Problems in Nonsmooth Domains*, Society for Industrial and Applied Mathematics (SIAM), Philadelphia, PA, 2011.
[22] F. Hecht, New development in freefem++, *J. Numer. Math.*, **20** (2012), 251-265.
[23] P. Henning and D. Peterseim, Oversampling for the multiscale finite element method, *Multiscale Model. Simul.*, **11** (2013), 1149-1175.
[24] U. Hornung, *Homogenization and Porous Media, Interdisciplinary Applied Mathematics*, vol. 6, Springer-Verlag, New York, 1997.
[25] T. Y. Hou and X. H. Wu, A multiscale finite element method for elliptic problems in composite materials and porous media, *J. Comput. Phys.*, **134** (1997), 169-189.
[26] W. Jäger and A. Mikelic, On the flow conditions at the boundary between a porous medium and an impervious solid, *Progress in Partial Differential Equations: The Metz Surveys*, **3** (1995), 145-161.
[27] V. Jikov, S. Kozlov and O. Oleinik, *Homogenization of Differential Operators and Integral Functionals*, Springer-Verlag, Berlin, 1994.

[28] I. Kevrekidis, C. Gear, J. Hyman, P. Kevrekidis, O. Runborg and C. Theodoropoulos, Equation-free, coarse-grained multiscale computation: Enabling microscopic simulators to perform system-level analysis, *Commun. Math. Sci.*, **1** (2003), 715-762.
[29] C. Le Bris, F. Legoll and A. Lozinski, MsFEM à la Crouzeix-Raviart for highly oscillatory elliptic problems, *Chinese Annals of Mathematics, Series B*, **34** (2013), 113-138.
[30] C. Le Bris, F. Legoll and A. Lozinski, An MsFEM type approach for perforated domains, *SIAM MMS*, **12** (2014), 1046-1077.
[31] E. Marušić-Paloka and A. Mikelić, An error estimate for correctors in the homogenization of the stokes and navier-stokes equations in a porous medium, *Boll. Unione Mat. Ital*, **10** (1996), 661-671.
[32] B. P. Muljadi, P. Degond, A. Lozinski and J. Narski, Non-conforming multiscale finite element method for Stokes flows in heterogeneous media. Part I: methodologies and numerical experiments, *Multiscale Model. Simul.*, **13** (2015), 1146-1172.
[33] J. Nolen, G. Papanicolaou and O. Pironneau, A framework for adaptive multiscale method for elliptic problems, *SIAM MMS*, **7** (2008), 171-196.
[34] D. Peterseim, Robustness of finite element simulations in densely packed random particle composites, *Networks and Heterogeneous Media*, **7** (2012), 113-126.
[35] E. Sánchez-Palencia, *Non-homogeneous Media and Vibration Theory*, Springer-Verlag, Berlin-New York, 1980.
[36] Z. Shen, Sharp convergence rates for Darcy's law, *Communications in Partial Differential Equations*, **47** (2022), 1098-1123.
[37] L. Tartar, Incompressible fluid flow in a porous medium-convergence of the homogenization process, *Appendix of* [35].

Received June 2022; revised August 2023; early access October 2023.